

Investigating Transient Overvoltage Produced by Switching Action on Long
Transmission Lines and Its Effect on Substations

by

Mohammed Mubashir Shaikh

A Thesis Presented in Partial Fulfillment
of the Requirements for the Degree
Master of Science

Approved August 2018 by the
Graduate Supervisory Committee:

George Karady
Jiangchao Qin, Chair
G. Thomas Heydt
Qin Lei

ARIZONA STATE UNIVERSITY

December 2018

ABSTRACT

Switching surges are a common type of phenomenon that occur on any sort of power system network. These are more pronounced on long transmission lines and in high voltage substations. The problem with switching surges is encountered when a lot of power is transmitted across a transmission line/network, typically from a concentrated generation node to a concentrated load. The problem becomes significantly worse when the transmission line is long and when the voltage levels are high, typically above 400 kV. These overvoltage transients occur following any type of switching action such as breaker operation, fault occurrence/clearance and energization, and they pose a very real danger to weakly interconnected systems. At EHV levels, the insulation coordination of such lines is mainly dictated by the peak level of switching surges, the most dangerous of which include three phase line energization and single-phase reclosing. Switching surges can depend on a number of independent and inter-dependent factors like voltage level, line length, tower construction, location along the line, and presence of other equipment like shunt/series reactors and capacitors.

This project discusses the approaches taken and methods applied to observe and tackle the problems associated with switching surges on a long transmission line. A detailed discussion pertaining to different aspects of switching surges and their effects is presented with results from various studies published in IEEE journals and conference papers. Then a series of simulations are presented to determine an arrangement of substation equipment with respect to incoming transmission lines; that correspond to the lowest surge levels at that substation.

To my father,

You taught me integrity and the value of honest work.

And to my mother,

You taught me to be compassionate even when everything else is the opposite.

And in memory of my mentor,

Dr. George Georgy Karady.

ACKNOWLEDGEMENTS

My sincere and heartfelt gratitude goes to my mentor and advisor, the late Dr. George Karady. I cannot thank you enough for all that you've taught me. This thesis itself was possible in the first place only because you believed that I can do it, and offered me the chance to work on it. May your soul rest in peace. I offer my sincerest prayers to your family after such great a loss.

I offer my thanks to Dr. Jiangchao Qin who took over as my committee chair, and my committee members Dr. Gerald Heydt and Dr. Qin Lei. You've been so supportive and understanding at such a critical stage in my thesis. My colleagues Aashiek Hariharan and Qianxue Xia were very supportive throughout my thesis. I cannot thank you guys enough.

Many thanks to my manager at Salt River Project, Dr. Snehal B. Dalal. Apart from the funding, you've given me an opportunity to work for such a great company. Your input towards my conference paper was amazing. I don't doubt that that is what got my paper accepted.

And finally, if I had to name someone without whom this thesis would not have been finished, it is my family. I thank the Almighty God from the bottom of my soul for giving me such amazing parents and siblings. My parents have been phenomenal in supporting me. They carried me through all my fears and insecurities and shaped me into who I am today. A mere paragraph in this thesis cannot do them justice. Despite being so far away from them, the only reason I could focus on my studies was because I had my sister and brother-in-law close by: Tooba Shaikh, you've been like a mother to me and

put up with my whims and selfishness all this time. I am really lucky to have you. Zeeshan Sayyed, you've been an amazing support, and I could always count on your advice. You're the best elder brother I can have. To my adorable niece Khadija and nephew Musa, I give the award of the cutest toddlers. You are just too cute.

TABLE OF CONTENTS

LIST OF TABLES	vii
LIST OF FIGURES	viii
LIST OF SYMBOLS	xi
CHAPTER 1 – INTRODUCTION	1
1.1 Problem description and project motivation	2
1.2 Thesis outline	3
CHAPTER 2 – LITERATURE REVIEW	4
2.1 Switching surges at ends of different transmission systems	4
2.2 Use of surge arresters for uprating a transmission line.....	5
2.3 Optimal surge arrester placement	12
2.4 Controlled switching of breakers to reduce switching surges	18
2.5 Surge arrester modeling and characteristics	23
2.6 Modeling of power transformers for transient behavior analyses	29
2.7 Conclusion	31
CHAPTER 3 – MODELING AND BASE CASE SIMULATIONS.....	33
3.1 Modeling.....	33
3.2 Configuration-A (base case development).....	36
3.3 Configuration-B (Switching at the terminating substation).....	42
3.4 Configuration-C (Switching at an intermediate substation)	45

CHAPTER 4 – DETAILED MODELING AND SYSTEM SIMULATION.....	48
4.1 Simulation.....	48
4.2 Key findings.....	50
CHAPTER 5 – CONCLUSIONS AND FUTURE WORK.....	52
5.1 Conclusions.....	52
5.2 Future work.....	53
REFERENCES	54

LIST OF TABLES

Table	Page
2.1 Effect of arresters on switching overvoltage	11
2.2 Line energization transients at line end	23
3.1.1 Transmission line details.....	34
3.1.2 Siemens 500 kV arrester characteristics	36
3.1.3 Siemens 230 kV arrester characteristics	36
3.2.1 Peak surge levels at transformer primary (line-neutral) for increasing line lengths.	38
3.3.1 Comparison of switching surge factors (line-neutral) with Table 3.2.1	43
3.4.1 Comparison of switching surge factors (line-neutral) with Table 3.2.1	46
4.1.1 Transmission line details.....	48
4.1.2 Simulation results.....	50

LIST OF FIGURES

Figure	Page
1.1 A standard 250/2500 μ s impulse waveform to study switching surges (IEC 60060-1)	1
2.1 No load energization of 400 km pure overhead system.....	4
2.2 Flowchart for surge arrester selection and optimal location.....	7
2.3 Phase to neutral switching overvoltage profiles	8
2.4 Coronado-Silver King 500 kV SSF study.....	9
2.5 (a) I-V characteristics of different surge arresters, (b) Three-phase energizing overvoltages without resistors.....	11
2.6 (a) Global risk of network for two voltage profiles, (b) Global risk of network for two BSLs.....	14
2.7 Line energization transients at sending end	15
2.8 Line energization transients at receiving end.....	16
2.9 Voltage profiles for surge arresters installed at optimum point.....	17
2.10 Voltage profiles for a surge arrester rated 372 kV.....	18
2.11 Model for analyses of CB switching of no-load 400 kV transmission line	19
2.12 TRV for regular switch off. Highest transient on phase A, $U_{L1} = 758$ kV	20
2.13 Distribution of TRV between breaking chambers	21

2.14 Distribution of TRV in CB chambers after installing grading capacitors	21
2.15 Line energization overvoltage with uncontrolled switching.....	22
2.16 Line energization overvoltage with controlled switching.....	22
2.17 Frequency dependent surge arrester model recommended by IEEE	24
2.18 Typical V-I characteristics of a MOV disk	24
2.19 Comparing simulated results to ATP/EMTP for an 8 μ s half cycled surge current	25
2.20 Proposed wide-range model of surge arrester	26
2.21 Response of test ZnO block to high frequency voltage under varying temperature .	27
2.22 Flowchart for genetic algorithm used in [9]	28
2.23 Equivalent winding capacitance network in a Y- Δ (HV-LV) transformer	31
3.1 Tower geometry used in simulations	34
3.2 Transformer model used for simulations	35
3.2.1 Configuration-A circuit representation	36
3.2.2 Voltage waveform at transformer primary (line length is 57.13 km, source voltage is 525 kV). Red waveform represents source voltage (phase-A) and blue waveform is voltage at transformer primary (phase-A).....	39
3.2.3 Simulation with surge arrester placed at bus-2	39
3.2.4 Expanded PSCAD model.....	40

3.2.5	Overvoltage waveform at end of line-2 for length = 1027 km	41
3.3.1	PSCAD model representation for Configuration-B	43
3.3.2	Comparison of line-neutral voltage waveforms obtained in the two cases	44
3.4.1	PSCAD model for case 3.4	45
3.4.2	Overvoltage waveform at bus 4 with: line-1 = 57.13 km, and line-2 = 500 km.....	47
3.4.3	Overvoltage waveform at bus 4 with: line-1 = 500 km, and line-2 = 57.13 km.....	47
4.1.1	Detailed model for Chapter-4 simulations	49
4.1.2	Arrester energy curves showing initial energy discharge for (a) switching at bus 3, (b) switching at bus 4.....	51

LIST OF SYMBOLS

ANN	Artificial Neural Network
ANSI	American National Standards Institute
ATP	Alternative Transients Program
BIL	Basic Insulation Level
BSL	Basic Switching impulse Level
CB	Circuit Breaker
EHV	Extra High Voltage
EMTP	Electromagnetic Transients Program
FERC	Federal Energy Regulatory Commission
FOW	Front of Wave
$f(V)$	Probability density of overvoltage occurrence
$f_s(V)$	Density function of overvoltage at line end
GA	Genetic Algorithm
HWACT	Half-Wavelength AC Transmission
KCL	Kirchhoff's Current Law
KVL	Kirchhoff's Voltage Law
LiDAR	Light Detection And Ranging

MOV	Metal Oxide Varistor
NERC	North American Electric Reliability Corporation
P(V)	Probability of disruptive discharge
P _i	Probability of flashover at tower <i>i</i>
R _{global}	Global risk of failure
SFO	Slow Front Overvoltage
SRP	Salt River Project
SSF	Switching Surge Factor
SSFOR	Switching Surge Flashover Rate
TRV	Transient Recovery Voltage
UHV	Ultra High Voltage
V'	Voltage at which insulation has 50% probability of flashover
σ	Standard deviation

CHAPTER 1

INTRODUCTION

Voltage surges are a common phenomenon in a power network. Switching surges especially, occur with more frequency than any other type of surge. They are usually considered to be the most severe pollutant to the insulation of a power system and connected equipment. These surges differ from lightning surges and other types in their frequency, peak amplitude and most importantly, rise time of the wave front.

Typical switching surges have a frequency ranging from a few kHz to a few hundred kHz. They generally are slow rising waves with a front time of more than 10 μs . Even though their peak magnitude might be lesser than that of lightning surges, they discharge huge amounts of energy. This is because the duration of these transients is much higher than lightning or other types of surges. This energy can cause severe damage to the equipment insulation, and potentially damage the equipment itself. The figure below shows a standard switching impulse waveform (as per IEC 60060-1) that is used for insulation testing in high voltage laboratories.

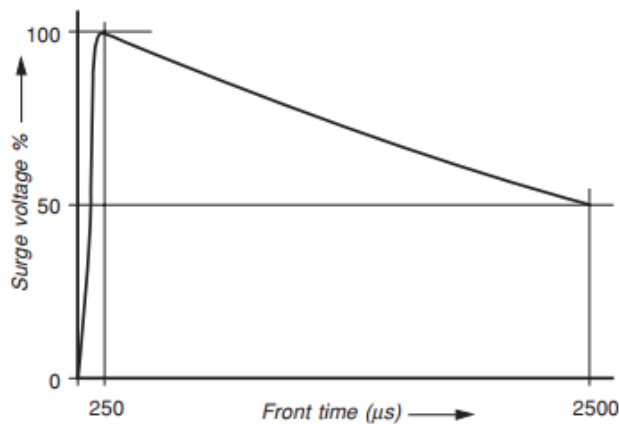


Fig. 1.1 – A standard 250/2500 μs impulse waveform to study switching surges [24]

There is a third category of voltage surges called very steep or front of wave (FOW) that also originate from breaker/recloser operation. They are extremely fast rising surges with very short waveform durations. Their front time maybe as small as $0.1 \mu\text{s}$ or even less (IEC 60071-1). Due their very short duration the amount of energy discharged is also very small, but since the rate of rise of voltage is extremely high they can damage small portions of conductors and insulators. This type of surges sometimes originate from restriking breaker contacts or a quick reclosing of high voltage equipment. This, combined with the switching transient that usually follows a breaker operation or the transient that happens when there is trapped charge on a line, can cause severe damage and further complicate matters. But in this project, these transients are not simulated and only the long-duration switching transients are studied.

1.1 Problem description and project motivation

In [3] SRP authors studied switching surge effects on a 500 kV transmission line and determined optimal locations along the line where surge arresters can be placed to meet NERC requirements. However, the effect of existing arrester units on switching surges was not studied. Many utility companies install surge arresters at substation entrance and at the terminals of important equipment like transformers. The Apparatus Engineering Department of a major utility company in Arizona is interested in investigating the usefulness of existing arrester units at substation entrances and equipment terminals. A transient study of the utility's network with appropriate simulations is required to achieve this goal.

1.2 Thesis outline

In chapter 2 a detailed discussion is presented in the form of a literature review covering topics such as switching surges, surge arresters, transformer and arrester modeling for transient analysis. This literature review investigates the topics relevant to this thesis as individual works presented by various authors. Apart from throwing some light on these topics for the reader, this literature review is a discussion about what work has already been done in these areas, and what scope remains.

Chapter 3 discusses the modeling aspect of this thesis, as recommended by IEEE and IEC standards. Then the problem is broken down into 3 main circuits or “configurations” and each is investigated in depth to determine the transient behavior of the corresponding circuit. Various conclusions are derived which are then applied to the final circuit developed in chapter 4.

Chapter 4 models the HV system of a major utility company according to the provided data and a PSCAD simulation model is developed. Points of interest noted in chapter 3 are applied to this model and the behavior of the system is explained based on these points. Finally, conclusions and scope of future work is presented.

CHAPTER 2

LITERATURE REVIEW

2.1 Switching surges at ends of different transmission systems, and reduction methods

In [1] the authors discuss the energization of long EHV (400 kV) mixed overhead-cable lines on no load. Since most lines in a power system exist as a mixture of overhead and cables, different combinations of overhead lines and cables are discussed and simulated, with each case containing at least 3 segments. These simulations are then analyzed from a transient aspect and from a quasi-steady state aspect also.

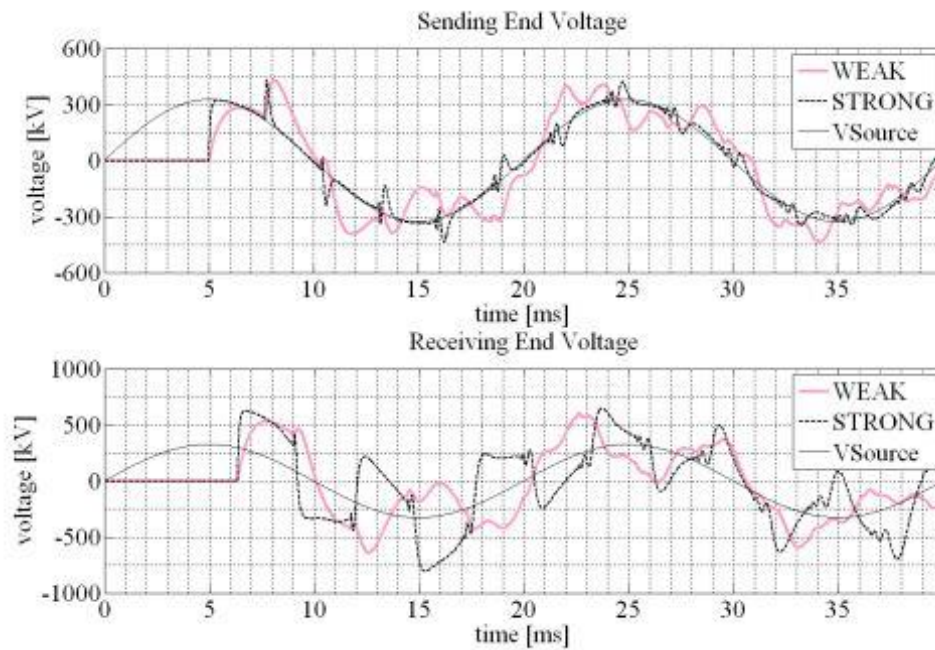


Fig. 2.1 – No load energization of 400 km pure overhead system

a) sending-end voltage b) receiving-end voltage ([1], Fig. 6)

The different line configurations that were simulated had a large difference of length in their first and last segments, in order to determine the configuration with the best end switching. These simulations were carried out with shunt reactors connected to the lines for reactive power compensation.

The total line length considered was 400 km with an overhead length of 320 km and cable length of 80 km (in different combinations). These simulations were later verified with calculations by determining the travelling wave reflection and refraction coefficients.

In one particular case, the whole configuration consisted just of one single stretch of overhead line with no load and shunt reactors. It was found that in this case, both sending end and receiving end voltages had lower damping than other configurations due to the absence of cable attenuation effect. The maximum switching overvoltage in this case was found to be 437 kV at the sending end and 807 kV at the receiving end.

2.2 Use of surge arresters for uprating a transmission line

Surge arresters can be used for uprating a transmission line too. Due to increasing power demand, there is a need to transmit increased power over longer distances.

Uprating an existing line is often a good and cost-effective option compared to laying a new line. In [2] and [6] the authors discuss how surge arresters are a good way to deal with the increased switching overvoltage that result from increased voltage ratings and lower clearances. For a long EHV transmission line, the severest switching surges occur during 3-phase reclosing when there is already trapped charge on the line. This usually happens after the clearing of a three phase or single-phase fault. Such trapped charge can

remain on the line for several seconds, hence, surge arresters must be installed to subdue the following switching transients.

In [2], a single circuit 220 kV transmission line is considered which was updated to 400 kV without any change in phase clearances. The impulse withstand voltage of the glass insulator was measured to be 790 kV. This setup was modeled in EMTP-RV and simulations were performed to obtain the $U_{2\%}$ values (the phase-neutral voltages having a 2% probability of being exceeded) along the line during multiple 3-phase reclosing operations of the breaker.

This overvoltage probability profile was calculated for cases corresponding to line without any surge arresters, line with surge arresters at ends and line with multiple surge arresters at optimal locations. The maximum switching surge value was found to be 4.7pu, which is 2658.7 kV (peak value), after 500 switching operations were simulated using statistic switches in EMTP-RV.

After installing surge arresters along the line using the iterative procedure in fig. 2.2, a significant reduction in switching overvoltage is obtained, as per the following overvoltage vs length curves.

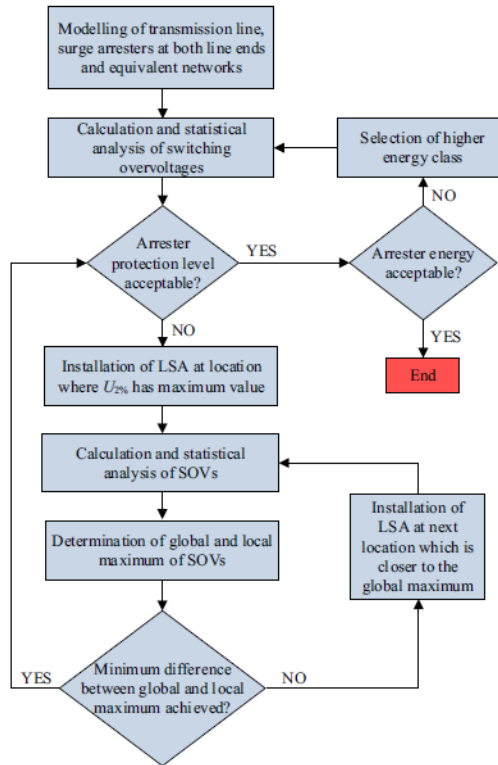


Fig. 2.2 - Flowchart for surge arrester selection and optimal location [2]

In [3], the authors from SRP and ABB investigate the effect of new NERC regulations on transmission lines' reliability, and discuss the effect of installing high energy surge arresters on a specific 500 kV SRP transmission line. NERC's new system requires a general review of ratings to make sure that design conditions and actual field conditions of high voltage transmission lines match, primarily in terms of clearance and switching surge factor (SSF) calculations of that network.

As already seen, installing surge arresters is a cost-effective way to reduce switching surges on a line and hence, increase its capacity for power transfer without any sort of increase in conductor clearances. Surge arresters can be installed without much

labor cost, and there is no need for line outage since installation can be carried out on a live line.

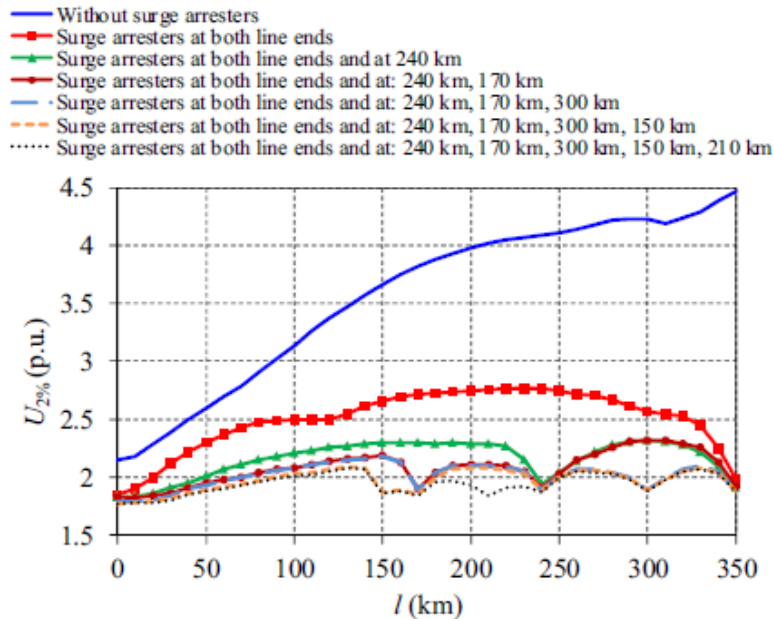


Fig. 2.3 - Phase to neutral switching overvoltage profiles [2]

In this case, SRP's 500 kV Coronado-Silver King line was considered which is 180 miles long. Line clearances were determined using LiDAR equipment mounted on a helicopter. For simulation, the line was represented by a frequency dependent model, and line arrester was modeled using manufacturer's data (Siemens). The surge arrester was a high strength polymer type with an energy handling capability of $13 \text{ kJ kV}_{\text{MCOV}}^{-1}$, and this rating was tested in accordance with the IEEE/ANSI std. C62.11-2012. This surge arrester was rated for duty cycle voltage of 420 kV and through an iterative optimization process, three sections were placed along the line length at 60, 108 and 137 miles from the line start.

The insulation was designed for a 98% withstand capability, and after 100 switching operations, the following results are obtained (SSFs calculated on a 550 kV base):

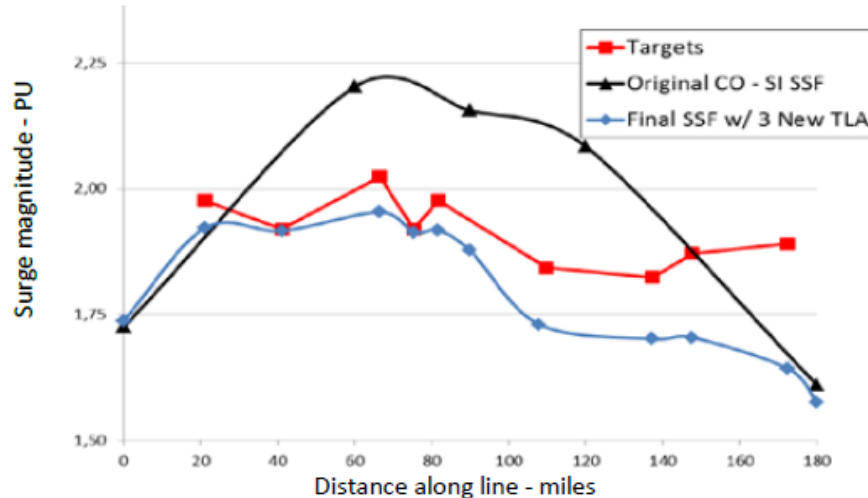


Fig. 2.4 – Coronado-Silver King 500 kV SSF study [3, fig. III-2]

It is clear from the above results that by installation of a few arresters, the maximum surge magnitude reduces by a considerable amount – down from over 2.2pu to 1.8pu. This can potentially help transmission operators satisfy NERC’s requirements of line clearances based on SSF reduction.

However, it is still left to see that by what particular arrangement of surge arresters at line ends (substations) can the SSFs be further reduced, without having to install additional units along the length.

In [4], the authors discuss the effects of parallel resistors and different surge arresters on a long UHV line. The line under consideration is a double circuit 1000 kV

line and is modeled using PSCAD/EMTDC. It was simulated in different modes (double circuit, one circuit grounded, one circuit ungrounded) and under different overvoltages (three phase energizing, single phase reclosing) using various surge protection arrangements (with parallel resistor, with different types of surge arresters and a combination of both).

Here, installing parallel resistors across circuit breakers was the primary overvoltage protection, and the usefulness of these resistors was seen by simulating the line with and without parallel resistors. The switching overvoltages with 98% probability were determined for different line sections through simulation. The most severe surge occurs when the longest section of line was simulated under single phase reclosing and it was found to be 1.80 pu (here, 1 pu = $1100 \text{ kV} * \sqrt{2}/\sqrt{3}$). Using parallel resistors this overvoltage was reduced to less than 1.59 pu.

One interesting observation noticed in the simulations was that when surge arresters were used on a parallel-resistor protection scheme on the line (at line ends only), under single-phase reclosing transient, the results were not much different than when only parallel resistors were used (table 1). This is because in single phase overvoltage conditions, parallel resistors consumed most of the transient energy and the arresters hardly had any effect [4]. But using surge arresters as a standalone option at line ends (without parallel resistors) under three-phase energization transients resulted in a significant reduction of overvoltage (less than 1.55pu, fig. 5).

Table 2.1 – Effect of arresters on switching overvoltages [4, table 4]

Type of overvoltage	Arrester	Switching overvoltage (p.u.)	
		Double-circuit	One-circuit ungrounded
Three-phase energizing	#1	1.59	1.64
	#2	1.54	1.60
	#3	1.49	1.56
	#4	1.48	1.55
Single-phase reclosing	#1	1.30	1.43
	#2	1.29	1.39
	#3	1.27	1.33
	#4	1.30	1.33

Another observation from this table is that the arresters work better with lower residual voltages. Arrester #1 is the commonly used UHV arrester in China, arrester #2 has 5% lower residual voltage, arrester #3 has 10% lesser residual voltage, and arrester #4 is a controllable arrester unit. Their I-V characteristics are given in fig. 2.5 (a).

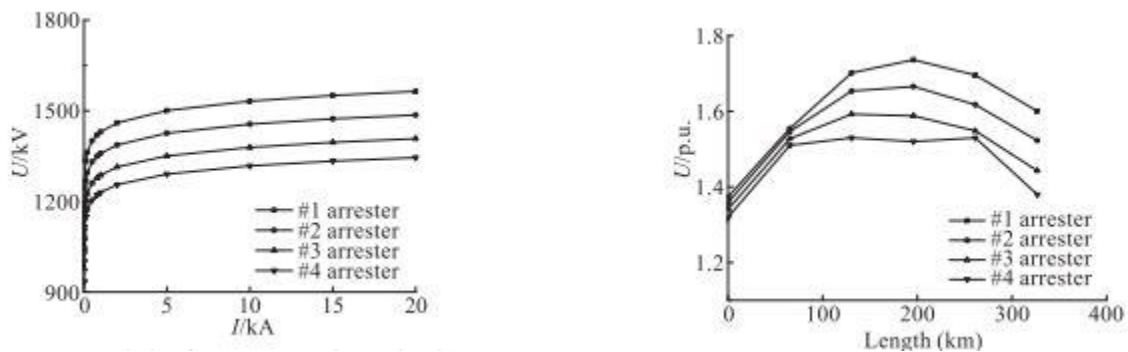


Fig. 2.5 (a) I-V characteristics of different surge arresters, (b) Three-phase energizing overvoltages without resistors. [4, fig.1, 2]

As previously seen, parallel resistors or “pre-insertion resistors” are traditionally used to prevent switching surges on long EHV and UHV lines, as the primary protection

method. But in recent years, there have been trends to find alternatives to pre-insertion resistors due to their inherent disadvantages and difficulty of use. A common alternative has been to use surge arresters along the line (at nodes determined by simulations and studies) or even at the line ends.

2.3 Optimal surge arrester placement

[5] and [7] employ an artificial neural network (ANN) to estimate the peak overvoltage values and calculate the global risk of failure. After that, a genetic algorithm (GA) is used to find optimal surge arrester locations to minimize this risk in [5].

$P(V)$ is the probability of disruptive discharge and is obtained by using the statistical switches of EMTP/ATP which generate the statistical distribution of switching surges at defined nodes (since there is no known function that directly gives the statistical distribution of surges).

$$P(V) = \frac{1}{\sigma \cdot \sqrt{2\pi}} * \int \exp \left[\frac{-(V-V')^2}{2\sigma^2} \right] dV \quad - (2.1) [5]$$

V' is the voltage at which the insulation has a 50% flashover probability.

$f(V)$ is the probability density of overvoltage occurrence and is a normal density function.

Then the risk function is just half of the multiplication of these two functions, and then integrating it from the minimum value of overvoltage to the maximum value.

The Switching Surge Flashover Rate (SSFOR) is calculated for n towers as –

$$SSFOR = \frac{1}{2} \int_{Eo}^{Em} [1 - \prod_{i=1}^n (1 - Pi)] * fs(V) dV \quad - (2.2) [5]$$

P_i is the probability of flashover at tower i , $f_s(V)$ is the density function of overvoltage at open end of the line. Then, the global risk of failure is just the average flashover rate of all lines in the network.

$$R_{\text{global}} = \frac{1}{N} \sum_{i=1}^N SSFOR_i \quad - (2.3) [5]$$

An ANN (Feed Forward Multilayer Perceptron architecture) is designed and tested with supervised training to compute these equations for different possible positions of surge arresters, and give the peak overvoltage and global risk of the network. The inputs to this ANN are the nodes of interest of the line, which may be suitable candidates for installing surge arresters.

Then a genetic algorithm (GA) is used to determine optimum locations for surge arrester installation that minimize the global risk to the network. GAs are computing methods for solving constrained and unconstrained optimization problems that are based on natural selection of individuals (or chromosomes). A GA repeatedly modifies a population of individual solutions until the best solution in the solution space is reached. Here, the GA minimizes the risk function in eqn. (2.3).

This optimization procedure was applied to a case study on Iranian southeast 400 kV network. There are 4 lines (3 sections in each line) and one generating station, and all other equipment has been ignored. To simulate the worst case the surge arresters at line ends were not modeled, radial lines were assumed to be open and the line was energized with trapped charge on it. Out of the 12 candidate nodes, surge arresters will be modeled on 5 of them as determined by the optimization procedure. A step-wise voltage profile

and a flat profile along the lines is obtained. The following figure (Fig. 6 (b)) shows the global risk when the basic switching impulse level (BSL) is 1050 kV or 950 kV.

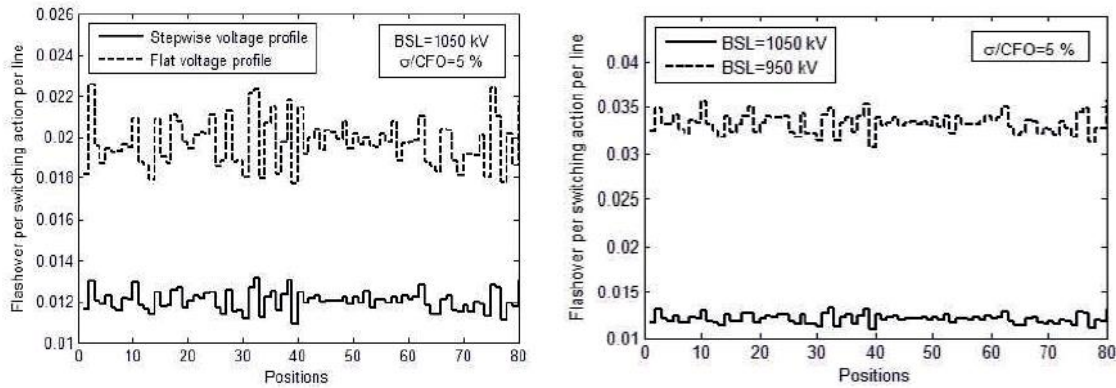


Fig. 2.6 – (a) Global risk of network for two voltage profiles, (b) Global risk of network for two BSLs ([5], Fig. 5,6)

The proposed method determined the optimum positions of the surge arresters as nodes 3,4,5,7 and 9 with a predicted flashover rate per switching operation of 0.0102 [5]. An interesting observation is that the program placed the arresters on line ends as expected, to reduce the open end line transients and hence, the global risk.

Reference [8] discusses the energization transients on a 500 kV transmission line that has only two surge arresters (420 kV arrester); one at each end. The line length is modeled in Brazil and is 2600 km, which is a little more than half the wavelength corresponding to a 60Hz wave. In Brazil, there are huge distances between the hydro power sources located near the Amazon basin and the load centers. These large distances have inspired studies into the effectiveness of HWACT lines (Half Wavelength AC Transmission) in transporting power.

Reference [9] suggests that such lines are highly advantageous for distances around 2500 km for a 60Hz system, and cost considerably less than a conventional AC line and an HVDC line [10]. After calculation of all relevant line parameters for each line section, a PSCAD/EMTDC model was developed and simulated using only surge arresters in one case and using pre-insertion resistors in another case. The results of surge arrester-only simulation are shown below.

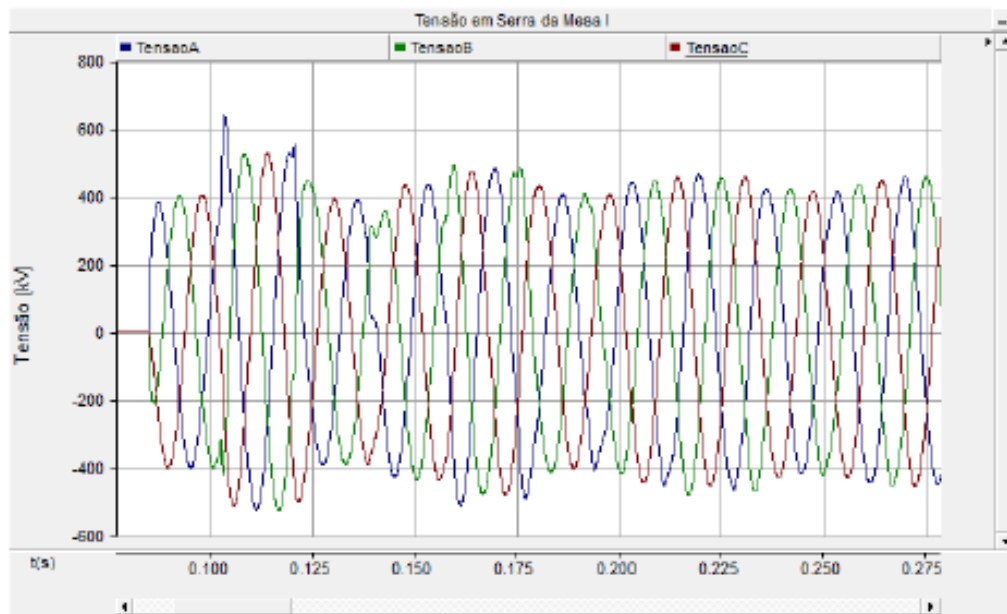


Fig. 2.7 – Line energization transients at sending end [8, Fig. 5]

It is seen that the highest overvoltage surges occur only at the ends of the whole line (at Serra da Mesa I and Bom Jesus da Lapa stations). This is because of the characteristic behavior of a half-wavelength line that the surges in the middle of the line are smaller than those at the line ends. It is noted that the best decrease in overvoltage is seen when surge arresters are used in conjunction with pre-insertion resistors. But the authors in [8] iterate that by using surge arresters with higher energy handling capabilities would be a more cost-effective solution.

Such transmission lines have a characteristic advantage of not requiring much reactive compensation and this hugely reduces the initial costs. Hence, this can be used as an effective solution for situations where such long distances are involved.

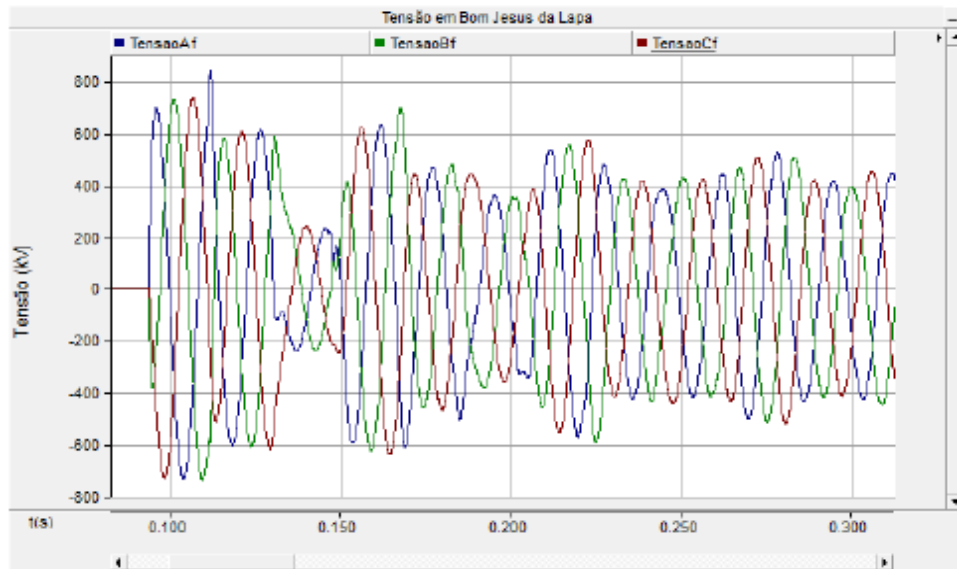


Fig. 2.8 – Line energization transients at receiving end [8, Fig. 7]

Another paper [11] discusses the switching overvoltage reduction along a 400 kV, 200 km long line belonging to the Iranian national grid. Primarily, line energization transients are modeled here using EMTP for simulation and CYMFAULT for calculating Thevenin equivalent parameters of the line model. The line under investigation connects the Isfahan and Soormag power plants. Three phase autoreclosers are also included in the model to get the worst switching instance (closing at max voltage instant with max charge on the line). Protection level of the line is designed for 1050 kV. Simulation of the line shows that without using surge arresters along the line, switching surges have a high possibility of exceeding this limit.

For finding the optimum location of surge arrester, a conjecture is made here [11] that (for switching on one end of the line) the absolute maxima of the overvoltage reaches its minimum value when overvoltages on either side of the surge arrester are equal. Same is true for finding the sub-optimum point for the other end. The final optimum point of surge arrester installation is between these two sub-optimum locations.

For a surge arrester rating of 336 kV, the final optimum location (from the above method) was found to be 137.5 km away from the Isfahan substation. Fig. 2.9 shows the voltage profile along the line and it is observed that the maximum overvoltage is below the line's protection level.

Further simulations show that this obtained value of minimum overvoltage shows an increasing trend when surge arresters of higher voltage ratings are used. Fig. 2.10 shows the voltage profiles for surge arrester of rating 372 kV. Hence if these surge arresters are selected, the protection level has to be increased to handle the overvoltage.

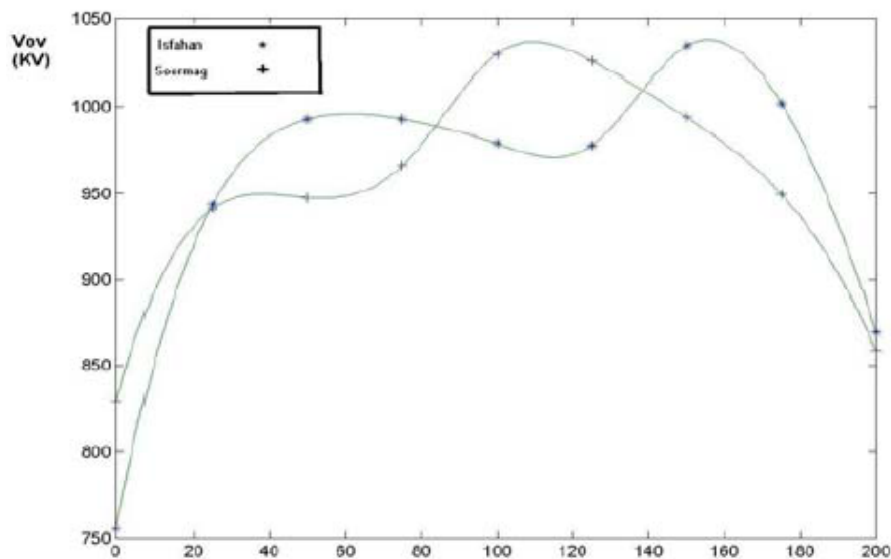


Fig. 2.9 – Voltage profiles for surge arresters installed at optimum point [11, Fig. 7]

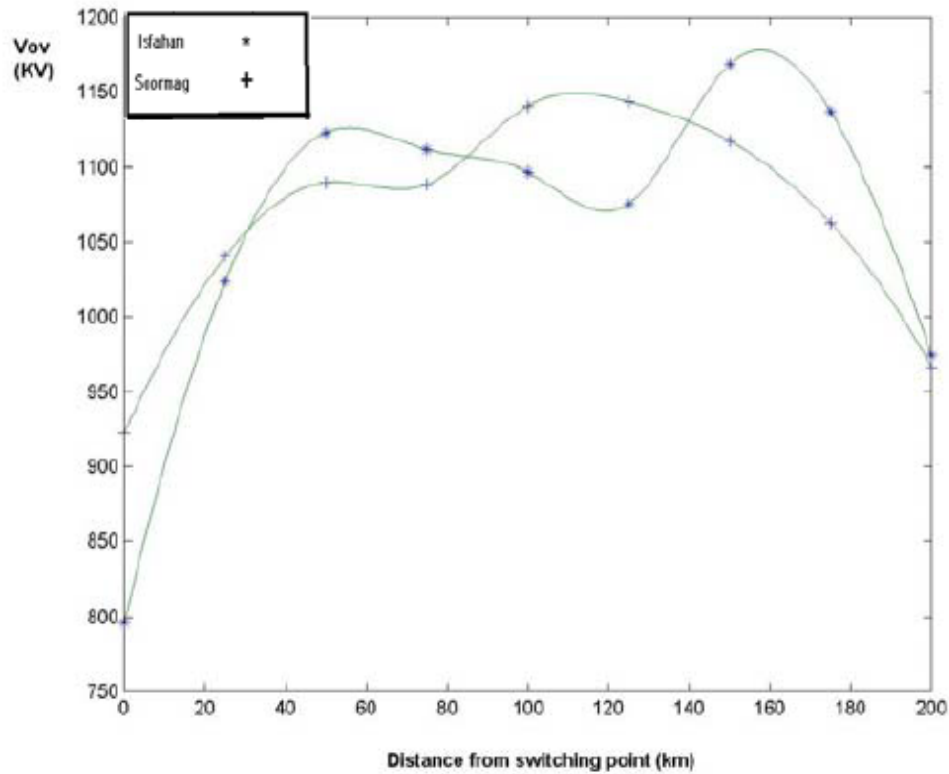


Fig. 2.10 – Voltage profiles for a surge arrester rated 372 kV [11, Fig. 13]

It was observed that using surge arresters by this method could provide a more flat voltage profile overall, which would eliminate the necessity of using pre-insertion resistors.

2.4 Controlled switching of breakers to reduce switching surges

Until now, all the methods discussed so far address the issue of reducing the surge voltages generated in the system due to various imperfect operations. But they don't address the root cause itself; the switching surges are primarily generated due to bad switching operations of the circuit breaker. One method of eliminating these overvoltage that is often discussed in literature is controlled switching of circuit breaker. Basically, in

this method the opening or closing operations of the circuit breaker are delayed so that the switching occurs at the optimum instant relative to the voltage phase angle.

Reference [12] investigates the overvoltages caused by controlled and uncontrolled switching of circuit breakers in high voltage circuits. It also discusses the energization and auto-reclosing transients on an unloaded 400 kV line of 231 km length. The model in EMTP-RV is shown in Fig. 2.11. The equipment in the substations is represented by surge capacitances, and the busbars and transmission lines according to a frequency dependent model.

First, the line switching off transients are studied without any control on the instant of switching in the breaker. The resulting transient recovery voltage on the breaker is shown in fig. 2.12.

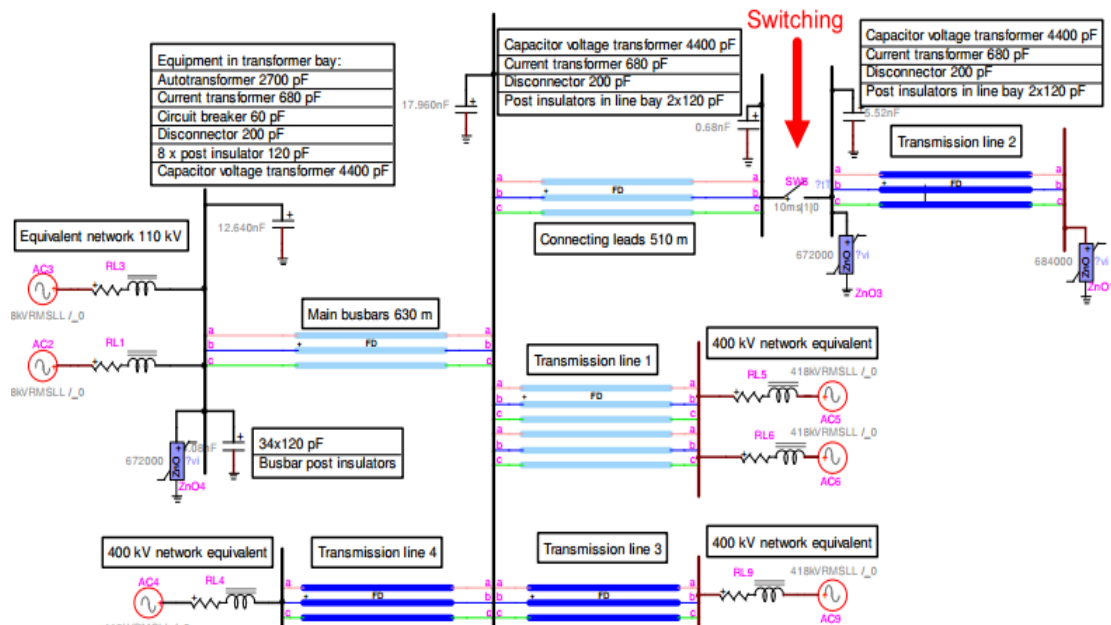


Fig. 2.11 – Model for analyses of CB switching of no-load 400 kV transmission line [12,

Fig. 14]

The circuit breakers were modeled as having two breaking chambers. Using this model, switching transients caused by uncontrolled switching of the line are shown below.

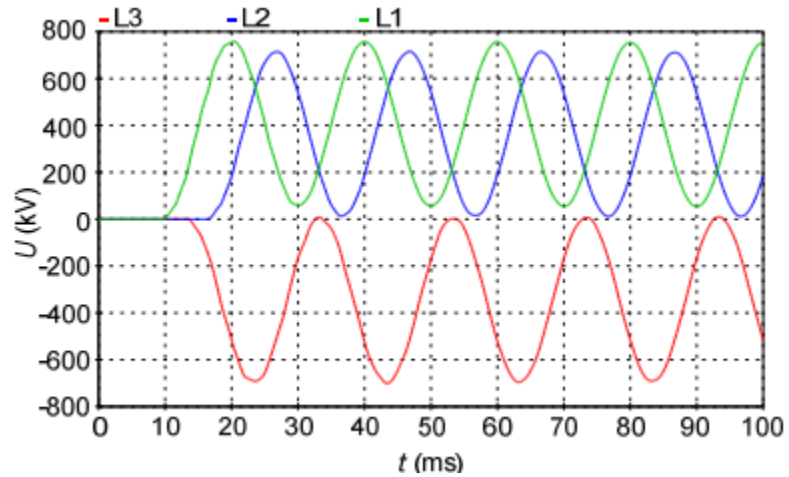


Fig. 2.12 – TRV for regular switch off. Highest transient on phase A, $U_{L1} = 758 \text{ kV}$

(2.32pu) [12, Fig. 17]

Such high TRVs are observed because capacitor voltage transformers are installed on both sides of the line. Hence the trapped charge discharges slowly. The highest voltage occurs on the phase that is switched off first due to coupling with other phases. Even inside the breaker, the voltage distribution is not uniform. Fig. 2.13 shows the uneven distribution of voltage in breaker of phase L1.

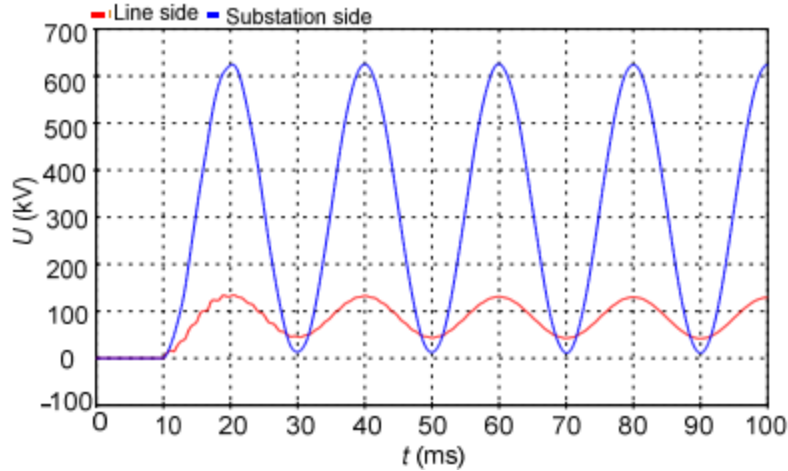


Fig. 2.13 – Distribution of TRV between breaking chambers. [12, fig. 18]

This distribution can be made more even by using grading capacitors. After simulations, a value of 500pF is selected and subsequent results are shown in Fig. 2.14.

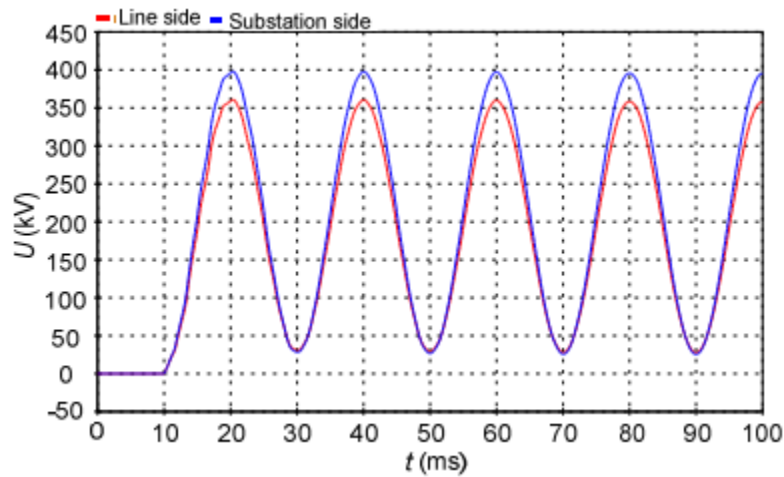


Fig. 2.14 – Distribution of TRV in CB chambers after installing grading capacitors. [12, fig. 19]

Similarly, the following figure 2.15 shows the worst case of line energization transients at the line end during uncontrolled switching of the breaker. In figure 2.16, line energization transients are shown during controlled switching operation of the breaker.

Controlled closing of breaker contacts in this case occurs at voltage zero-crossing instants. Table 2.2 summarizes the results of the simulation findings.

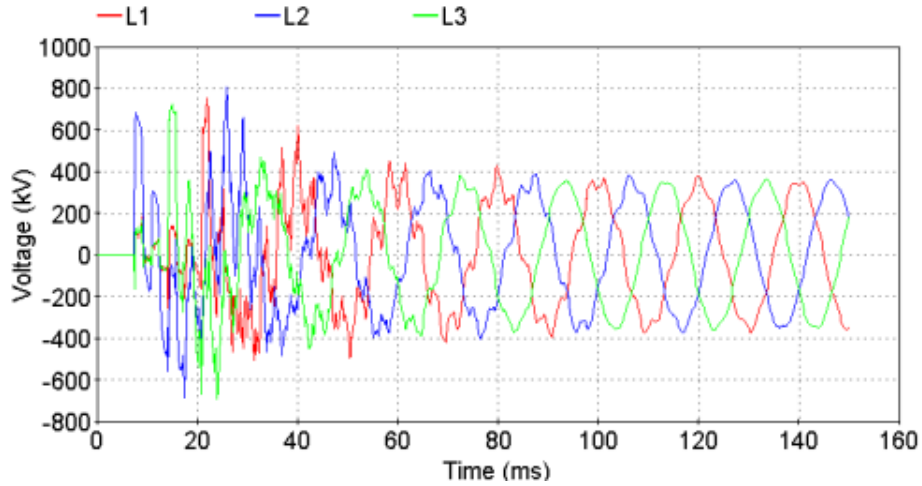


Fig. 2.15 – Line energization overvoltage with uncontrolled switching. [12, Fig. 21]

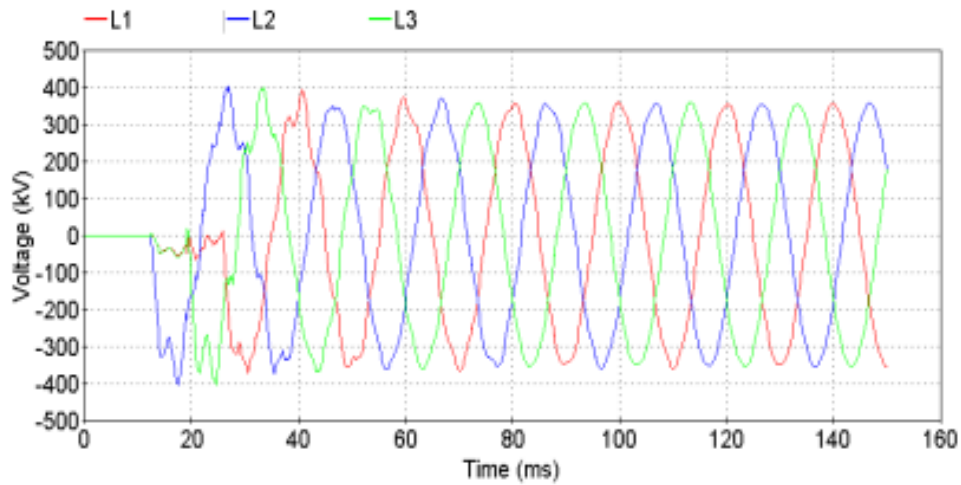


Fig. 2.16 – Line energization overvoltage with controlled switching. [12, Fig. 23]

Table 2.2 – Line energization transients at line end [12, Table III]

	Voltage amplitude (kV)					
	Uncontrolled switching			Controlled switching		
	U_{L1}	U_{L2}	U_{L3}	U_{L1}	U_{L2}	U_{L3}
Without surge arresters	752	803	723	392	401	397
With surge arresters	634	630	632			

2.5 Surge arrester modeling and characteristics

Now, we take a look at the characteristics of a surge arrester itself, i.e., what types of surge arresters are typically used, what type of common waveforms an arrester normally handles, and finally how to design and select different parameters through various methods.

Reference [13] describes a numerical model of very fast transient characteristics for surge arresters. The model here makes use of KCL and differential equations to solve for the arrester parameters on the IEEE recommended model, which is shown in figure 2.17. The surge arrester characteristics used here are that of a typical ZnO varistor and these characteristics are shown in figure 2.18.

The current in region 1 of the arrester is usually less than 1mA and is capacitive current. This is the region when the surge arrester operates in under normal conditions. The current in region 2 varies around 1kA or 2kA and is resistive. In region 3, the current varies anywhere from 1kA to 100kA and this is usually modeled by a linear relationship.

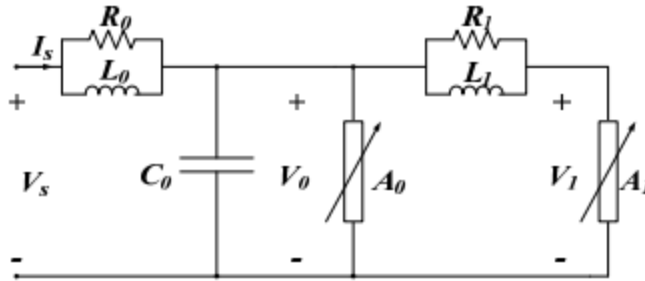


Fig. 2.17 [13, fig. 2] – Frequency dependent surge arrester model recommended by IEEE

[17]

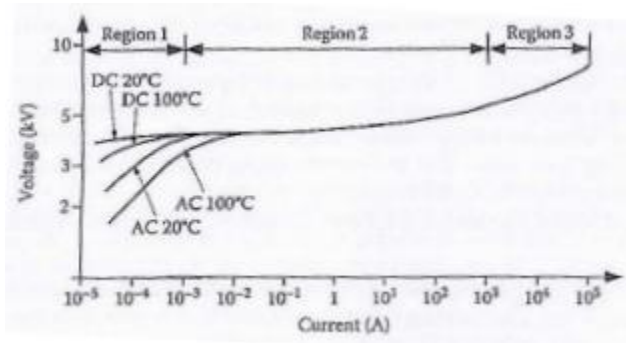


Fig. 2.18 – Typical V-I characteristics of a MOV disk [13, fig. 1]

KCL is applied to the model shown in fig. 2.17 and the subsequent equations are solved by using numerical methods like trapezoidal rule or Euler’s backward difference formula. The results are then simulated and compared in ATP/EMTP and Matlab’s PSB toolset.

Comparing this model’s results with simulated results for 8/20 μ s and 2/20 μ s Heidler’s surge currents shows that the numerical calculations in [13] and modeling is robust and accurate. A detailed comparison between the conventional and IEEE surge arrester models is made in [18].

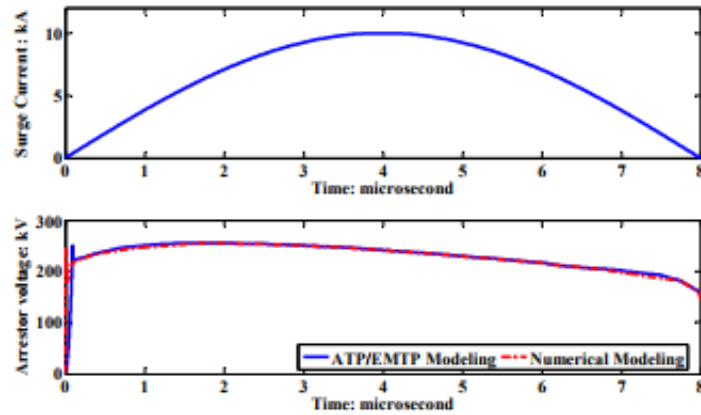


Fig. 2.19 – Comparing results to ATP/EMTP for an 8 μ s half cycled surge current [13]

On the other hand, [14] presents a model for a ZnO surge arrester that can be used in a large range of frequencies and magnitudes. This was developed and validated for each of the three regions shown in fig. 2.18, and furthermore from a database composed of voltage and current waveforms measured from tests on 12 different varistor units from 5 different manufacturers. These varistors were subjected to different voltage levels in the low current region, switching current impulses of 30/60 μ s, lightning current impulses (8/20 μ s) and fast front current impulses (1.5/26 μ s and 3/6 μ s).

When a surge arrester faces overvoltage transients, it operates in the non-linear region (region 2) wherein its behavior is predominantly resistive. In the high current region when the arrester is subjected to very fast transients, studies report a mostly inductive or dynamic behavior. At this time, the residual voltage of the arrester increases with the decrease in impulse front time. These varying operating ranges make accurate modeling of the arrester more complex, [14] proposes a model that represents all three stages and which is valid for a wide range of impulse frequencies and amplitudes. After

application of a number of test impulses in a laboratory set up, the following model was proposed.

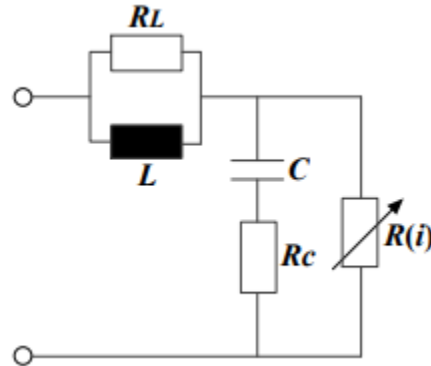


Fig. 2.20 – Proposed wide-range model of surge arrester [14, fig. 5]

The inductance L represents the magnetic field of the current flowing through the arrester, C represents the permittivity of the arrester under low current region of operation, and the $R(i)$ represents the non-linear characteristics of the arrester under region 2 of operation. The dependencies of these parameters and their calculation is done in [14].

As a special point of interest, [15] studies the effectiveness of using surge arresters to protect a 3 phase, 20 kV cable from vacuum CB operation on inductive loads. Although the voltage level of interest in [15] is different from what is discussed here, the setup holds quite a lot of similarity to the overall objective of this review.

Reference [16] investigates the response of an MOV to high frequency surges as a method of determining the ageing of the unit, since most lightning strokes are in the MHz frequency range, while most switching surges lie in the kHz frequency range. The gapless

type arrester has a small leakage current flowing through it during normal operation. This current increases with increasing operating temperature of the arrester.

An experimental testbed is setup in a lab and a ZnO block is subjected to various pulses of varying frequencies (kHz to MHz) under a fixed temperature. This temperature is then increased and the resulting leakage current magnitude and phase angle is observed. From the following figures, it can be seen that leakage current at an elevated temperature of 58°C is almost 10 times higher than that at reduced temperature. The phase angle on the other hand, varies from 90° lead to zero with increasing frequency, corresponding to change in operating region from region 1 to 2. But this change reduces significantly when the temperature is increased.

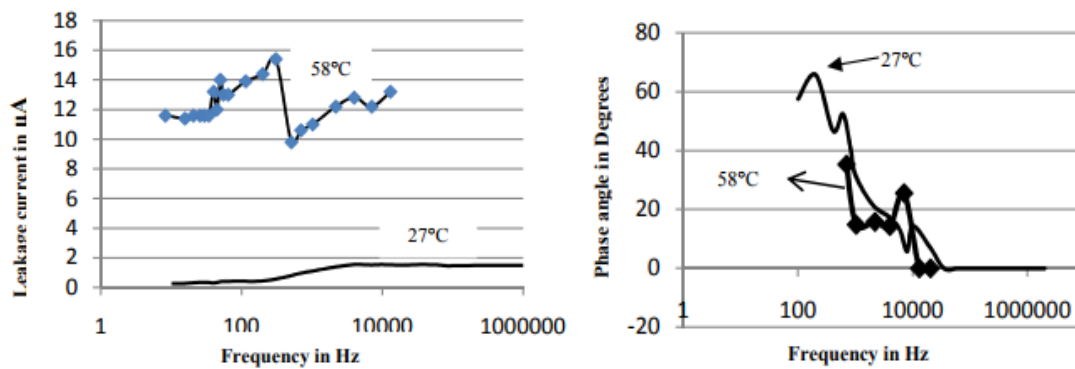


Fig. 2.21 – Response of test ZnO block to high frequency voltage under varying temperature [16].

For the design and parameter selection of a surge arrester, [19] proposes a genetic algorithm to solve for and optimize the selection of equivalent circuit parameters from the IEEE recommended surge arrester model, and also for two other similar models – the Pinceti-Gianettoni model and the Fernandez-Diaz model [19, fig 2-3].

Here, the error function is defined as the relative difference between the predicted residual voltage value in the arrester and the measured value from the manufacturer's data sheet. This error function is minimized. After representing the non-linear quantities A_0 and A_1 with piecewise linear functions from figure 18, KCL and KVL are used to derive the respective equations [19, (1)-(20)] containing the variables (respective resistances and inductances).

The following figure 2.22 from [19 fig. 4] shows the flowchart for the employed algorithm. This procedure is applied to each arrester equivalent circuit to compute the variable resistance and inductances.

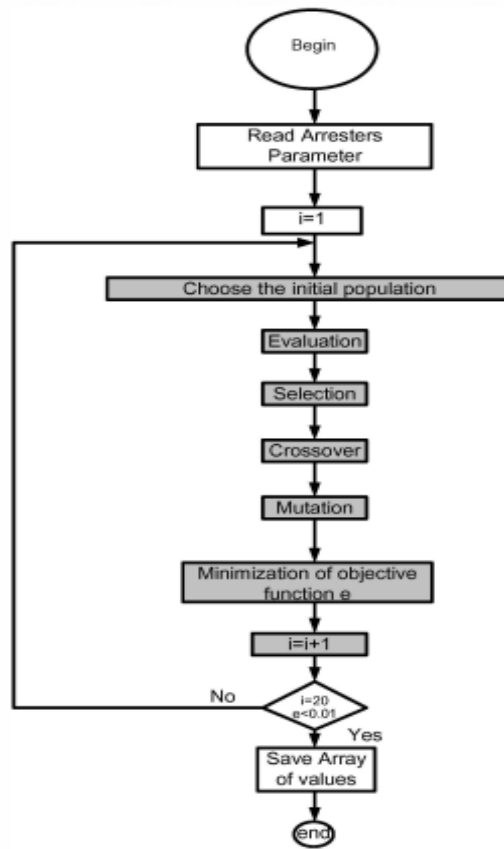


Fig. 2.22 – Flowchart for genetic algorithm used in [19]

The residual voltage was then calculated from the values given by this procedure, and the value from the datasheet. This method yielded an error of almost 0% when used on the IEEE recommended model and Fernandez-Diaz model, and an error value of 0.0067% in the residual voltage value calculated from the final, optimized parameter values. A good advantage pointed out by the authors is that results obtained are very accurate for a wide range of parameter values, compared to other optimization methods like simplex, Powell, and downhill (which strongly depend on initial values).

There are other attempts discussed in the literature to optimally select a surge arrester's parameters using other methods. [20] uses a complex, self-adaptive particle swarm optimization procedure, while [21] handles this task from a finite-element and heat transfer based method.

2.6 Modeling of power transformers for transient behavior analyses

Now we take a look at how power transformers are modeled when subjected to high frequency signals of switching surges. According to IEC 60060-1, a standard switching impulse has a front time of 250 μ s and falls off in thousands of microseconds (standard switching impulse is a 250/2500 μ s). Switching surges usually have frequencies in the kHz range (5-100 kHz) while lightning surges occur in the MHz range. In these ranges, the different capacitances in a transformer cannot be ignored and hence, the model should contain winding-winding and winding-ground capacitances.

Reference [22] proposes an equivalent winding capacitance network for transient analysis of a transformer subjected to surges with such frequencies. This model accurately represents positive and zero sequence winding capacitances. From a modeling

point of view, there are two main models that incorporate winding capacitances. The half-split method uses lumped parameters and is a more widely used model due to its simplicity and availability of parameter values. The second model is based on a distributed-parameter approach which neglects the winding magnetomotive force. Even though this method is more accurate, the parameters needed in the model are not easily available. The approach used in this paper determines lumped terminal capacitances while accounting for winding magnetomotive forces and core effects, thereby making the model suitable for transient analyses.

Two main and important component-parameters in the proposed model are the zero-sequence and positive-sequence capacitances. Assuming a linear voltage distribution along the windings and equal insulation gap between the winding and the adjacent surface (casing, transformer body or another winding), the zero-sequence capacitance is readily obtained from the standard dielectric tests conducted by the manufacturer.

But under normal operating conditions, the winding voltage profile with respect to ground and other windings is quite different from that in the dielectric test. This depends on factors like winding design and connection. Hence, the capacitive current from the voltage source and equivalent capacitance as observed from the source are also different.

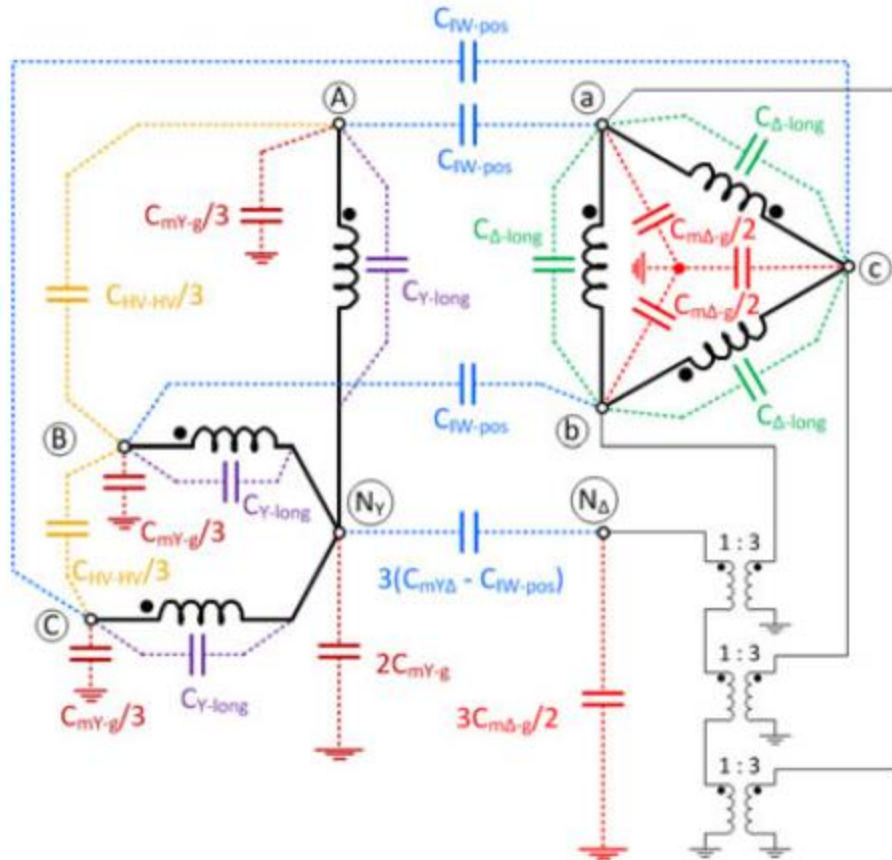


Fig. 2.23 – Equivalent winding capacitance network in a Y-Δ (HV-LV) transformer [22]

2.7 Conclusion

As seen from the above studies, switching surges present a very real danger to the power system under consideration and becomes the single most important factor during insulation coordination of a system above 400 kV. These switching surges occur frequently during any kind of circuit breaker operation or fault occurrence/clearing. To protect against this overvoltage, the insulation of the system can be upgraded to withstand the high surges, or pre-insertion resistors can be installed across breaker contacts to absorb the surge energy. However, both these methods are expensive and offer an ineffective solution to the problem. On the other hand, installing surge arresters at line

ends or at different points along the line is often a cheaper and easier solution. It can also be used when upgrading a transmission line becomes necessary to reduce the increased surge levels.

This project studies switching surge levels on different arrangements of substation equipment (breaker, transformer, surge arrester) with respect to incoming transmission lines. A PSCAD model is developed which will help study these factors in more detail, and in the context of actual lines and substation data belonging to a major utility company in Arizona. This will enable the utility to gain a much better insight into how a substation as a whole reacts to switching surges, and this will help during installation of protective devices (surge arresters) to protect substation equipment. The next section showcases simulations carried out in PSCAD/EMTDC (v4.6) that study certain scenarios of switching surge occurrence.

CHAPTER 3

MODELING AND BASE CASE SIMULATIONS

In this chapter, modeling of various circuit components is discussed, as recommended in [24]. Using these guidelines, simulation studies are performed to determine surge levels in three different circuit configurations. The three are then compared against each other to get a clearer understanding about switching surge levels in the model.

The simulations in this section are carried out with the following assumptions: there are no series/shunt compensating elements (reactors or capacitor banks) in the circuit, high switching surges don't result in insulator flashovers, and that there is no trapped charge in the line being energized. Also, it is assumed that the secondary side of the transformer at substation is open.

3.1 Modeling

3.1.1 Transmission lines

Overhead transmission lines are represented in subsequent simulations using PSCAD's frequency-dependent model, which is quite advanced in its representation. According to [24], a traveling wave model can be used, or a frequency-dependent model with a constant transform matrix or frequency dependent transform matrix may also be used. Hence, the PSCAD model selected for this study is sufficient. Line parameters are listed in Table 3.1.

Table 3.1.1 Transmission line details

Parameter	Value
Conductor type	Chukar, 1780 KCM, ACSR
Stranding	84/19
Average span (m)	304.8
Bundles, spacing (cm)	3, 45.7
No. of shield wires	2 x 7 #8 AW
Type, diameter (cm)	Alumoweld, 0.98

(Source: 500 kV line data from a major utility company)

This data is used to select the appropriate tower in PSCAD and model the transmission line definition. In this section, the following tower geometry is used for simulations.

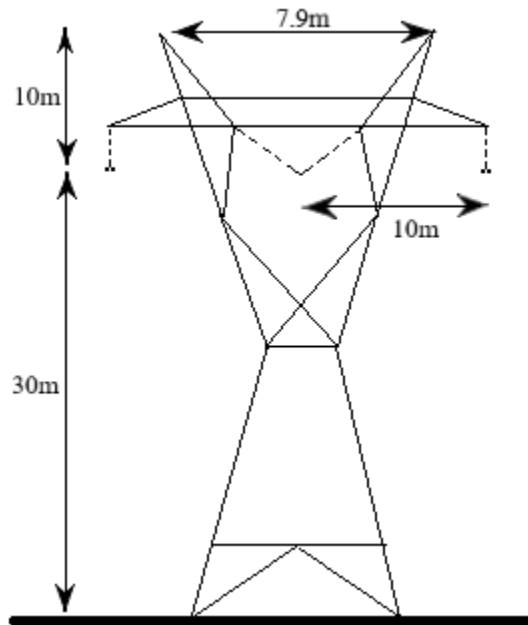


Fig. 3.1 – Tower geometry used in simulations (tower type is 3L2).

3.1.2 Transformer

According to [24], a high frequency transformer model can be used when studying slow front transient waveforms. Since the distributed winding-winding capacitance (C_{hl}) and winding-ground capacitances (C_{hg} , C_{lg}) are difficult to model accurately as they involve complex analyses, lumped parameters are used. Reference [24] recommends estimated values that usually prove sufficient for modeling purposes, and these values are used for simulation.

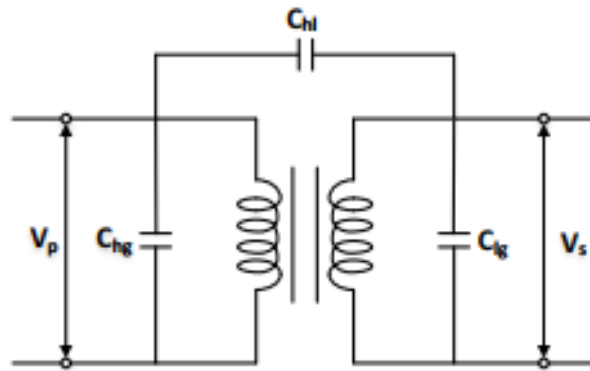


Fig. 3.2 – Transformer model used for simulations [23].

The transformer used in simulations in Section IV is modeled as a shell type, star-star autotransformer with winding voltages as 525 kV/230 kV and rated for 100MVA with neutral grounded. The HV winding is rated for a Basic Insulation Level (BIL) of 1425 and LV winding is rated for a BIL of 825. Core and hysteresis losses are included to avoid resonant behaviour.

3.1.3 Surge arrester

The surge arrester is modeled according to the datasheet of Siemens's 500 kV, 3EL2-class arrester. The characteristics are shown in Table 3.2 and Table 3.3 below.

Table 3.1.2 Siemens 500 kV arrester characteristics

3EL2	8/20 μ s				45/90 μ s		
I (kA)	5	10	20	40	0.5	1	2
V (kV)	930	989	1088	1187	801	821	860

Table 3.1.3 Siemens 230 kV arrester characteristics

3EL2	1/2 μ s	8/20 μ s				45/90 μ s		
I (kA)	10	5	10	20	40	0.5	1	2
V (kV)	458	406	432	480	544	346	354	372

Where,

I – maximum current amplitude (peak).

V – maximum discharge voltage (peak).

3.2 Configuration-A (base case development)

A simple PSCAD model is developed here to establish the base case for simulation. In this model, a PSCAD type-2 voltage source (525 kV) is connected via breaker to a long transmission line whose length is varied. This line is terminated at a substation bus (fig. 3.2.1).

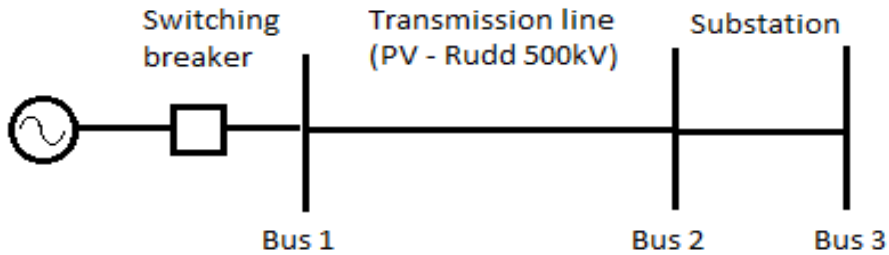


Fig. 3.2.1 – Configuration-A circuit representation.

The 525 kV/230 kV transformer is modeled using its capacitance model, since effect of winding-winding and winding-earth capacitances should not be ignored when conducting such transient studies. An estimate of transformer capacitance values is obtained from [24] (tables 5 and 6, page-37).

Another purpose of this simulation is to determine the critical line length of this specific circuit. A transmission line with its length equal to critical length yields drastically increased surge levels at its ends. Ideally it is equal to a quarter of the total wavelength of that line (wavelength of a 60 Hz system). The peak switching surges are tabulated in Table 3.2.1 for increasing line lengths. The worst case of switching is observed when breaker operation occurs at the crest of source voltage (for an unloaded line). To verify this, the simulation was repeated for successive time steps over a full cycle. This was done using a component in PSCAD called “multi-run”, which repeats a simulation by varying a specific quantity and outputs the maximum/minimum result.

Table 3.2.1 shows a general trend of increasing surge levels for longer lines, which becomes more pronounced for lengths greater than 500 km. For the circuit in figure 3.2.1 the critical length is determined to be 1227 km. Although this length is too large for any single line in the utility’s EHV network, the next case (Fig. 3.2.4) shows that this may not always be the case and one still needs to keep the critical line length in mind.

Table 3.2.1. Peak surge levels at transformer primary (line-neutral) for increasing lengths.

Line length (km)	SSF (pu)
100	2.01
200	1.99
300	2.08
400	1.99
500	2.34
600	2.69
700	3.01
800	3.25
900	4.49
1000	6.16

(Per unit calculations are on a base of 525kV, 100MVA)

Figure 3.2.2 shows the voltage transient for line length of 57.13 km, which is the actual length of Palo Verde – Rudd connection. For simplicity, only phase-A waveforms are displayed in the Fig. 3.2.2 and Fig. 3.2.3.

Figure 3.2.3 shows the maximum overvoltage that appears at bus-2 when a surge arrester is placed at that location. From this figure, a slight reduction in overvoltage is observed at the transformer primary terminals. The absolute value of peak surge reduced from 879.2 kV (fig. 3.2.2) to 753.14 kV (fig. 3.2.3). Also, the subsequent oscillations of the transient have been damped in within a cycle. This reduction is significantly more for longer line lengths.

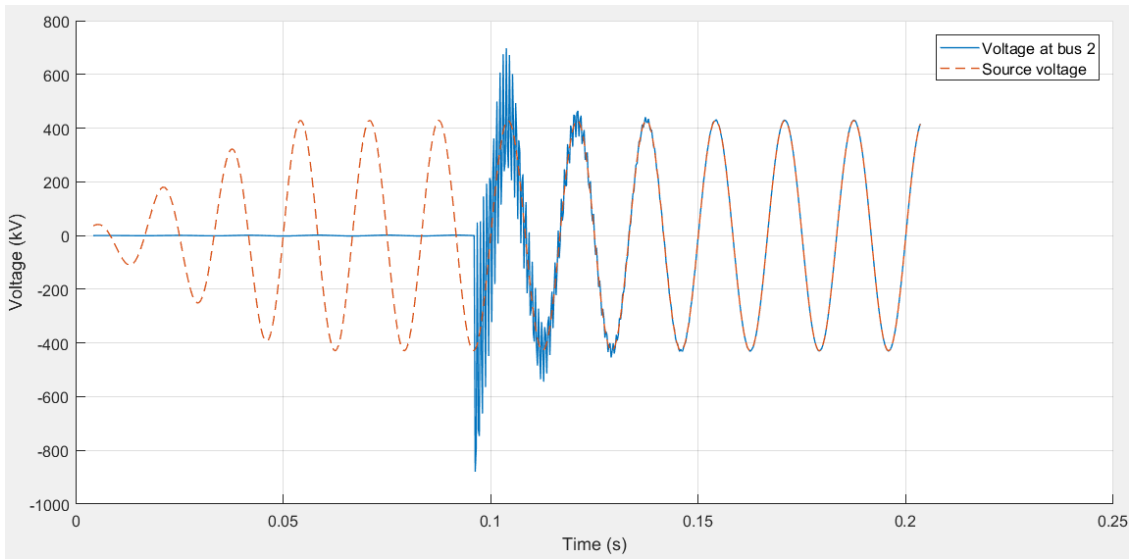


Fig. 3.2.2 – Voltage waveform at transformer primary without surge arrester (line length = 57.13 km, source voltage = 525 kV).

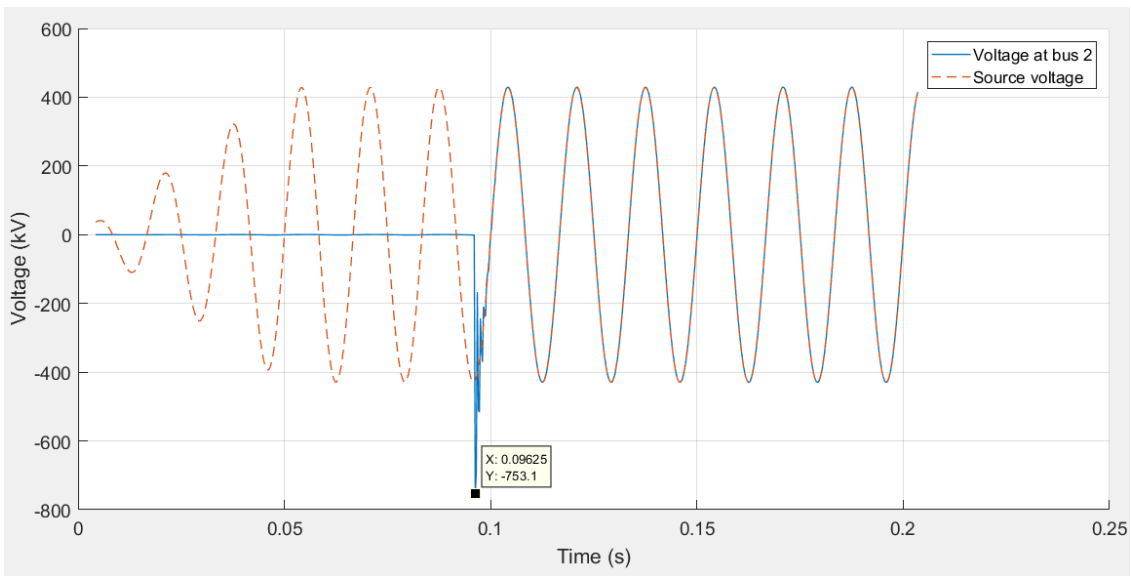


Fig. 3.2.3 – Voltage waveform at transformer primary with surge arrester (line length = 57.13 km, source voltage = 525 kV).

Modelling multiple lines terminated at the substation

Now, this PSCAD model is expanded to include more components. Another long transmission line is terminated at the substation bus, which is open circuited at its other end. A second 525 kV/230 kV transformer is added to the substation which is also open circuited at its secondary.

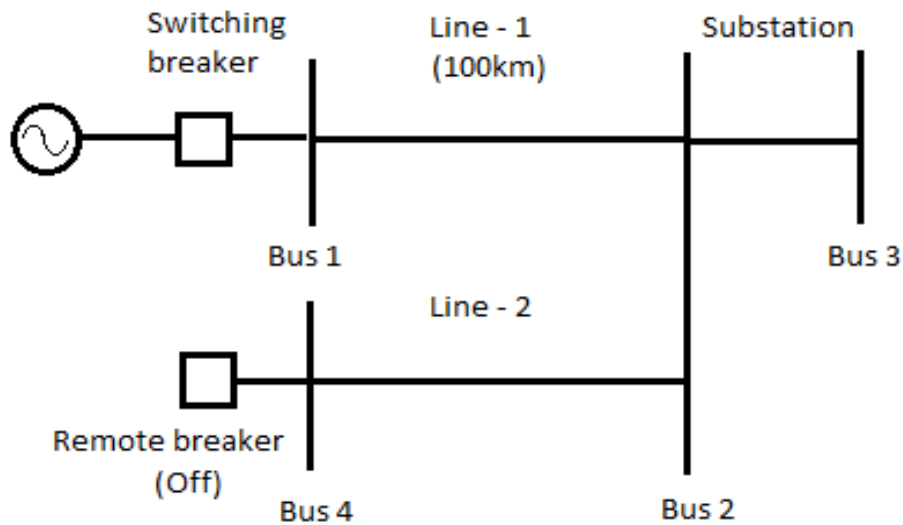


Fig. 3.2.4 – Expanded PSCAD model.

The new line (line – 2) is modeled using the same tower geometry and conductor specifications as line-1. Its length is varied in steps while line-1 is set to 100 km. The multi-run component is set to record the simulation where maximum overvoltage appears at bus 2.

An interesting observation is made: the critical length of line-2 is 1127 km. This, combined with length of line-1 gives a total of 1227 km, which is the critical length determined previously. The critical length in this particular setup remains unchanged, even when both lengths are further varied (as long as they add up to 1227 km).

This is an important conclusion. Although the critical length is too large for a single line to have, under the assumptions of this simulation it can be distributed among multiple transmission lines terminated at the same substation. Fig. 3.2.5 shows the substation voltage when the total length of both lines is near critical (line-1 is 100 km, line-2 is 1000 km).

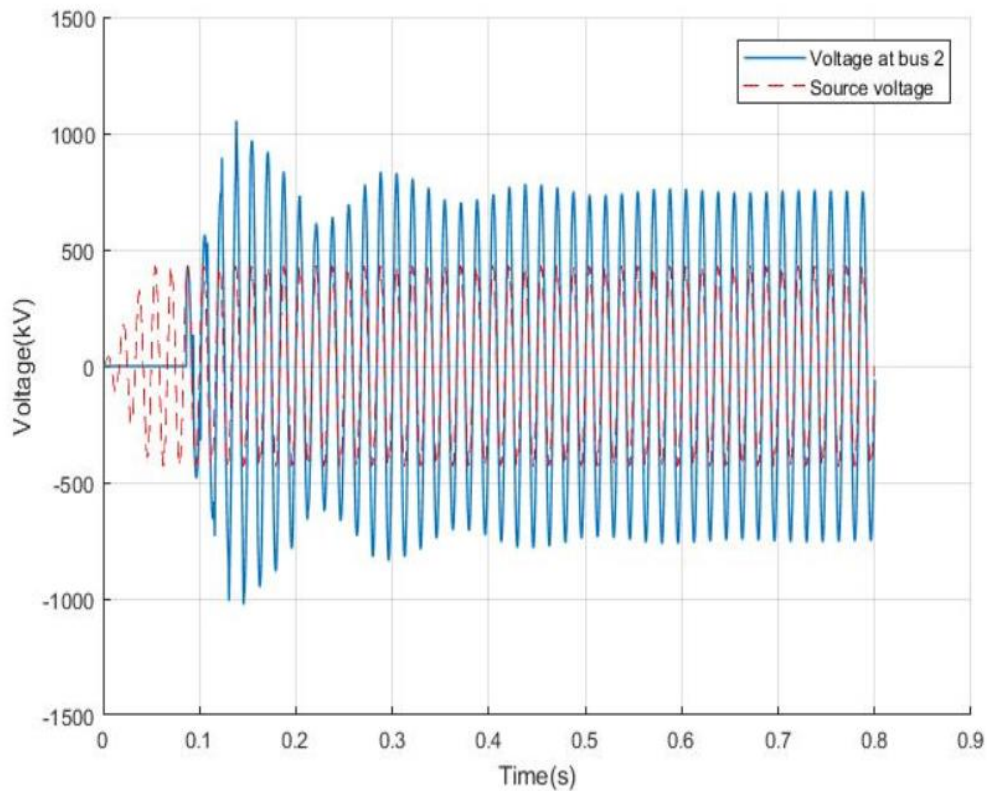


Fig. 3.2.5 – Overvoltage waveform at end of line-2 for length = 1027 km.

From the above observations, it is concluded that the critical length of a given line is a function of its tower geometry and conductor arrangement. Varying the tower geometry in this simulation gave a different value of critical length that the one obtained earlier.

At critical length there is a huge increase in voltage levels in the whole system. This is because travelling voltage waves get reflected from bus 4, and travel back to bus 2 where they add up to give the result shown in Fig. 3.2.5.

The next two sub-sections describe simulations for Configuration-B and Configuration-C. One of the main concerns listed in the project proposal is to determine a relative arrangement of substation equipment (circuit breaker, line, transformer and surge arrester) that results in a significantly lower peak surge at the substation. Usually, this issue is linked to the optimal placement of a surge arrester within a substation: to place a unit each in front of valuable substation equipment (transformers, capacitor and reactor banks, etc.) or to place it only at the substation entrance (bus). There are various issues/advantages associated with both approaches. The following simulations are run to investigate these scenarios.

3.3 Configuration-B (Switching at the terminating substation)

This type of switching is an event that occurs frequently in substations. Typically, this happens when a spare transformer or a transformer on standby is switched on to a live bus, at which multiple lines are terminated. From the substation's perspective, the switching is a local event.

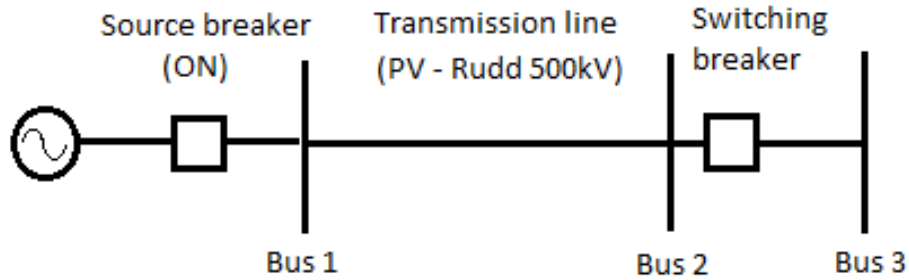


Fig. 3.3.1 – PSCAD model representation for Configuration-B.

Simulating this case shows that this arrangement yields surge levels that are far lower than those observed in Configuration-A. To get a clearer picture, peak values of resulting overvoltage in this case are compared against peak overvoltage values from case 3.2 (Fig. 3.2.1) and are tabulated in Table 3.3.1.

Table 3.3.1. Comparison of switching surge factors (line-neutral) with Table 3.2.1.

Line length (km)	Peak absolute SSF in this case (pu)	Peak absolute SSF in Configuration-A (pu)
100	1.01	2.01
200	1.04	1.99
300	1.09	2.08
400	1.15	1.99
500	1.29	2.34
600	1.42	2.69
700	1.69	3.01
800	2.16	3.25
900	2.60	4.49
1000	4.51	6.16

(Per unit calculations are on a base of 525kV, 100MVA)

As seen from above table, peak surge values are significantly lower than those obtained in case 3.2 for equal line lengths. But the waveform shapes are very different for

the two cases. Consider Fig. 3.3.2 showing overvoltage waveforms for the two cases for a line length of 500 km.

The overvoltage waveform obtained in case 3.2 (dashed line) shows an initial transient, which then settles to a steady state value after several cycles. But the waveform obtained from this case (solid line) does not show any transient behavior. It has already settled to its steady state value after a very short time, and doesn't show an oscillatory behavior like the blue waveform. This can be attributed to the relative difference in impedance present in the circuit after the breaker. In case 3.2, there was the transmission line impedance in addition to the small transformer reactance ($X=0.1pu$), whereas in this case only the transformer reactance is present after the breaker.

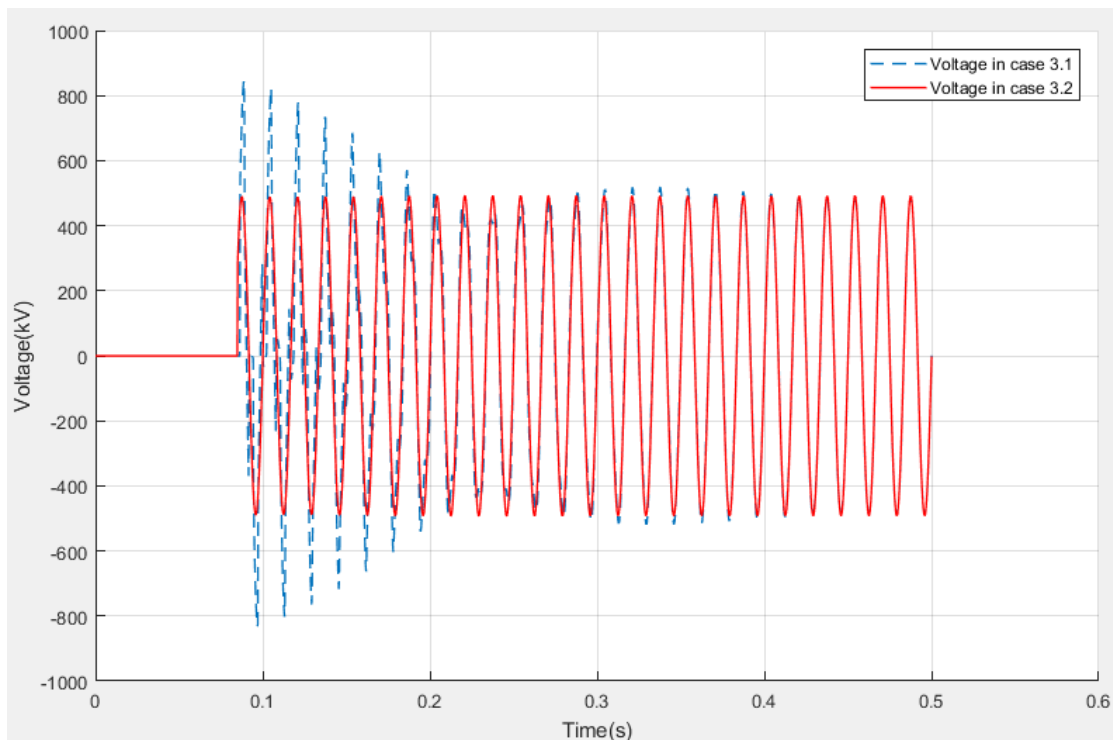


Fig. 3.3.2 – Comparison of line-neutral voltage waveforms obtained in the two cases.

3.4 Configuration-C (Switching at an intermediate substation)

In this simulation, the substation where switching occurs is located at some distance from the generating station and from the location where resulting surges are measured. Figure 3.4.1 shows the PSCAD model of this simulation.

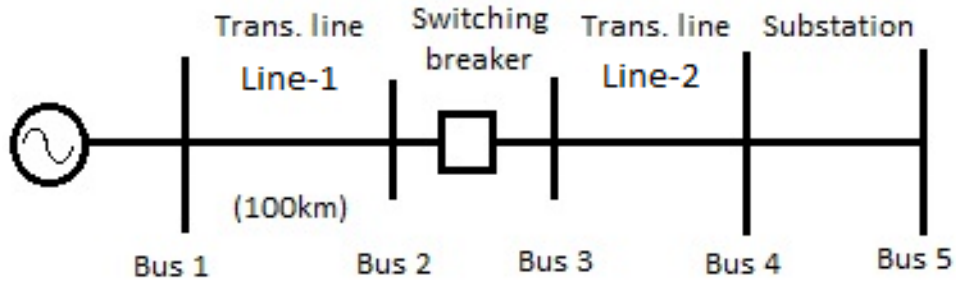


Fig. 3.4.1 – PSCAD model for case 3.4

The length of line-1 is kept constant at 100 km and length of line-2 is varied to observe the surge waveform at bus 4. As will be seen later, the transient behavior in this case will be influenced by length of line-2. Table 3.4.1 shows absolute value of peak surge at bus 4 and compares it against peak surge values in Table 3.2.1 for equal (total) line lengths.

From Table 3.4.1 it is seen that both cases yield similar surge levels. In fact, for higher transmission line lengths, the results are practically the same (within a small margin). This is because this circuit is quite similar to the circuit in case 3.2. It was observed in case 3.3, that the length of transmission line before the switching breaker does not contribute much to the surge level at the end of the line. In this case, the second segment of transmission line is made longer than the first segment. It is this segment that

dictates the surge level and waveform at the substation bus, and hence this circuit behaves in the same way as the circuit in case 3.2.

Table 3.4.1. Comparison of switching surge factors (line-neutral) with table 3.2.1.

Line length (km)	Absolute peak SSF in this case (pu)	Absolute peak SSF in Configuration-A (pu)
100	1.91	2.01
200	1.97	1.99
300	2.07	2.08
400	1.98	1.99
500	2.33	2.34
600	2.69	2.69
700	3.01	3.01
800	3.62	3.25
900	4.49	4.49
1000	6.15	6.16

(Per unit calculations are on a base of 525kV, 100MVA)

The reverse is also true; if the length of line-2 is made smaller than line-1, the peak surge incident on bus 4 is lower and the transients also settle faster. This is illustrated in Figures 3.4.2 and 3.4.3 below.

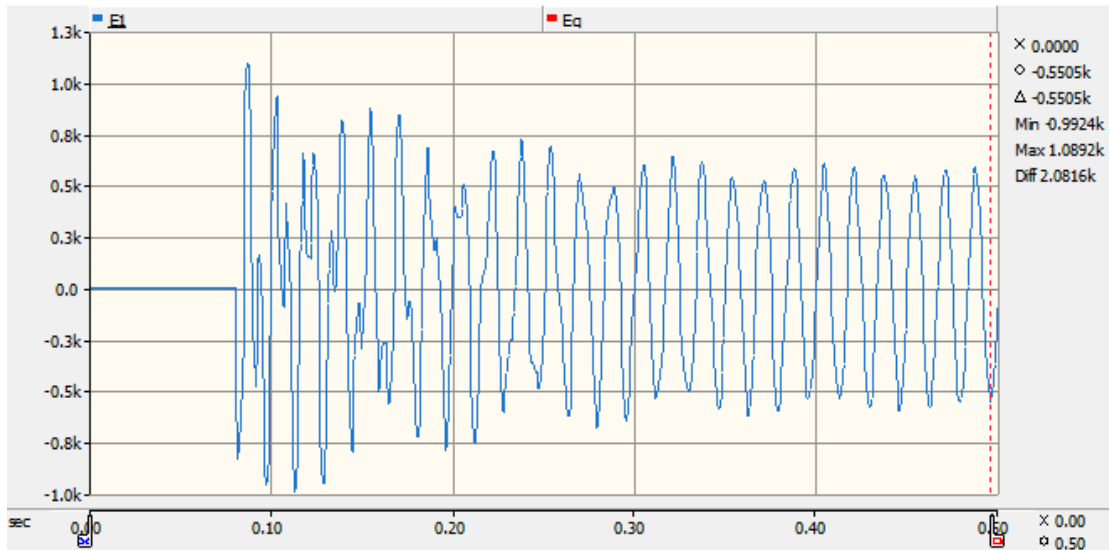


Figure 3.4.2 – Overvoltage waveform at bus 4 with: line-1 = 57.13 km, line-2 = 500 km.

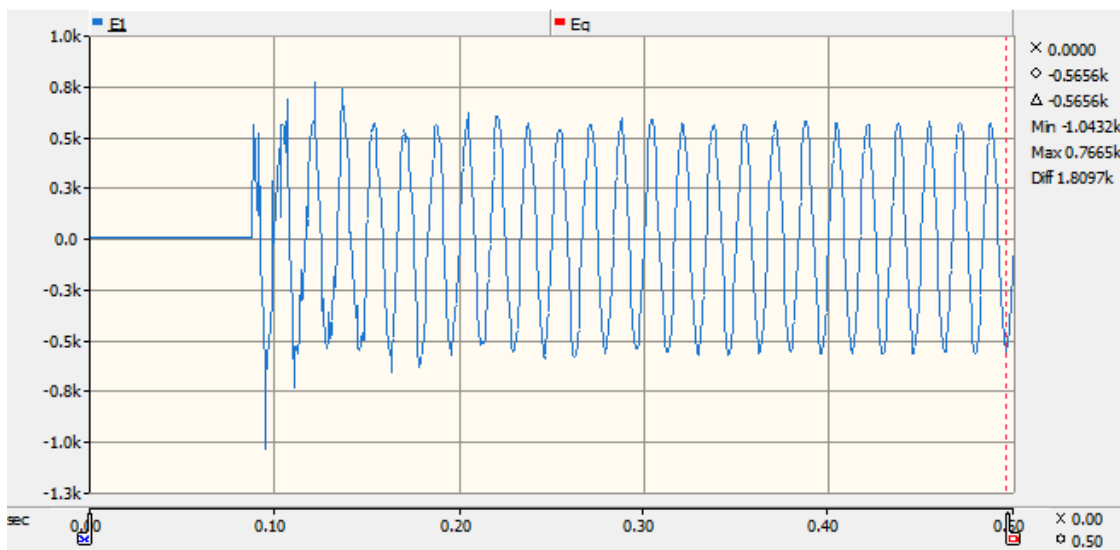


Fig. 3.4.3 – Overvoltage waveform at bus 4 with: line-1 = 500 km, line-2 = 57.13 km.

In this arrangement too, the critical length can be distributed between the two segments. But regardless of the fact which transmission segment is longer, it remains the same.

CHAPTER 4

DETAILED MODELING AND SYSTEM SIMULATION

4.1 Simulation

In this section, the simulation model is expanded to include nearby substations and transmission lines up to two buses away from the line of interest. This model is used to study switching behavior corresponding to configurations described in the previous section and study the surge levels at various points in the system. Here, each segment of the line of interest line is modeled with individual PSCAD definitions, since each segment has different tower geometries. Table 4.1 shows the details of the new transmission lines included in this model.

Table 4.1.1 Transmission line details

From	To	Voltage (kV)	Segment	Length (km)	No. of circuits	Tower type
Palo Verde	Rudd	500	1	15.0	1	3L1
			2	14.8		3L Concentric
			3	3.7		3L Vertical
			4	5.9		3L Concentric
			5	13.4		3L Vertical
			6	4.3		3L Vertical
Palo Verde	West Wing	500	1	72.6	2	3L1
Palo Verde	Hassayampa	500	1	5.0	3	3L1
Rudd	Liberty	230	1	14.5	1	3L1
Rudd	White Tanks	230	1	4.8	1	3L1
Rudd	Orme	230	1	12.9	2	3L1

The simulations in this section are carried out with similar assumptions as in chapter-3: there is no trapped charge on the transmission lines being energized and that high surges do not cause insulator/arrester flashover. Moreover, it is assumed that HV breakers at remote substations (buses 1, 2 and 7 in Fig. 4.1) are open, thus, the respective transmission lines are unloaded. As a sanity check to make sure the model is working without any errors, voltage regulation is calculated for a reasonable load connected to one of the 230 kV buses. It is found to be within an allowable margin (<10%). The circuit modeled for this case is shown in Fig. 9.

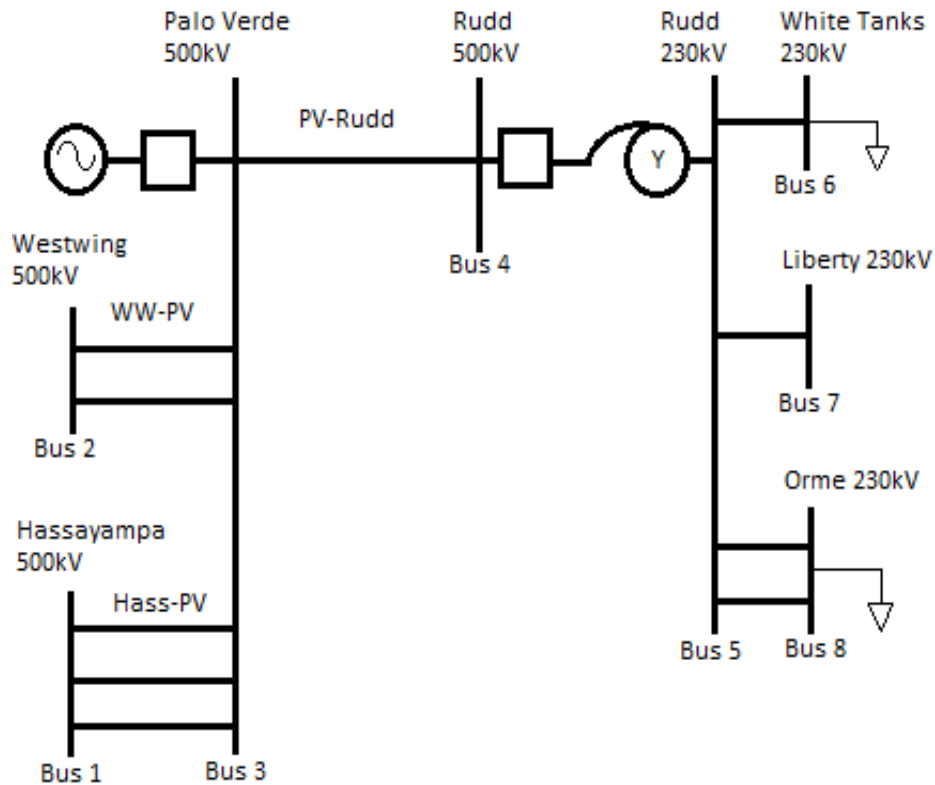


Fig. 4.1.1 – Detailed model for Chapter-4 simulations.

In Chapter-3 it was observed that surges originating from breaker operation at a remote location are higher in magnitude than those originating due to local switching

operation, because of the line capacitance. For the model developed in this chapter, two switching scenarios are studied: breaker closing at bus 3, and breaker closing at bus 4.

These correspond to Configurations A and C described in Chapter-3 respectively.

Simulations are performed by connecting an arbitrary load (70 MW and 25 MVAR) at bus 6 and bus 8 each. Then a surge arrester is connected at bus 4 and simulations are repeated to observe surge levels at various points in the model. The results are summarized in Table 4.2.

Table 4.1.2 Simulation results

SSF (pu)	Switching at bus 3		Switching at bus 4	
	<i>Without arrester</i>	<i>With arrester</i>	<i>Without arrester</i>	<i>With arrester</i>
At bus 4	1.59	1.47	1.10	1.10
At bus 6	1.47	1.37	1.03	1.03
At bus 8	1.47	1.37	1.03	1.03

(Per unit calculations are on a base of 525kV, 100MVA)

4.2 Key findings

For a 500 kV system, the IEEE Std 1427-2006 [25] recommends minimum clearances when SSFs are greater than or equal to 2.0 p.u. But the maximum SSF observed here is 1.59 p.u. at bus 4 when switching occurs at bus 4. Hence, the switching surge levels in this system are determined to be within limits. Also, from Table 4.1.2, it is seen that surges generated from switching at bus 4 are significantly lower in magnitude as compared to those generated when breaker at bus 3 is switched. From Fig. 4.1.2, it can be seen that surge arrester energy discharge is also within limits.

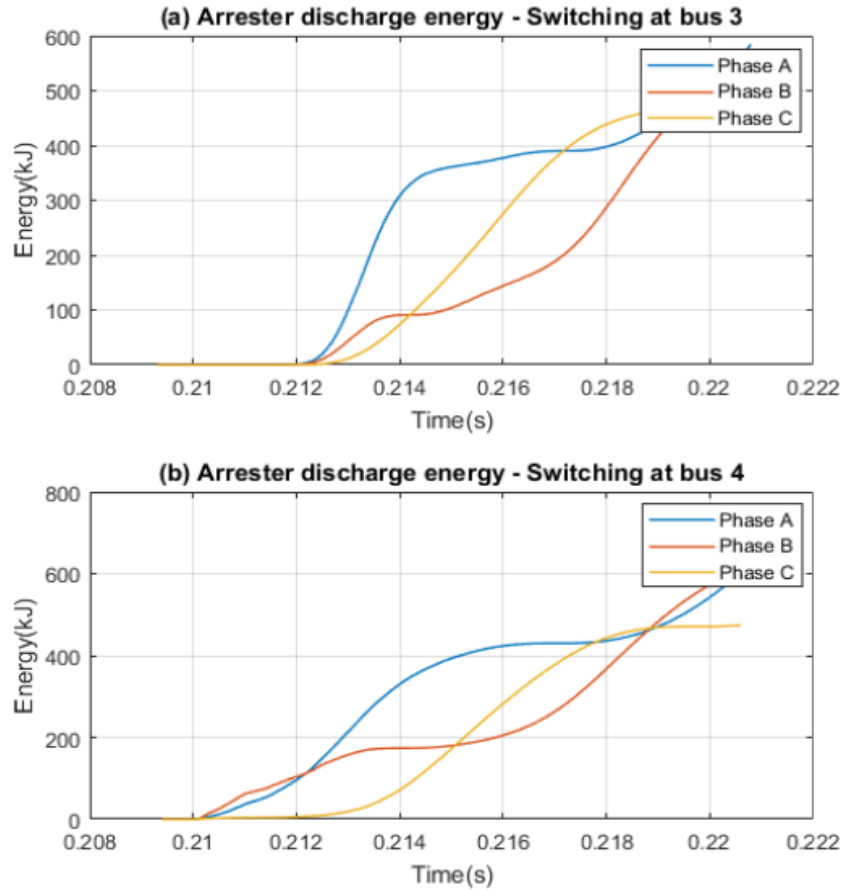


Fig. 4.1.2 - Arrester energy curves showing initial energy discharge for (a) switching at bus 3, (b) switching at bus 4.

The sub-case of Configuration-A (Fig. 4) is also examined for this model: if a new line is terminated at bus 3, what would its critical length be that would result in drastically increased surge levels in the system? A new, unloaded line with tower geometry same as bus 2 – bus 3 transmission line is terminated at bus 3. It turns out that the critical length of this new line is 1110 km, corresponding to which the SSF at bus 4 rises to 4.81 p.u.! If this line is terminated at bus 4 instead, its critical length is determined to be 1055 km. The location at which the switching occurs does not affect surge levels in this case.

CHAPTER 5

CONCLUSIONS AND FUTURE WORK

5.1 Conclusions

A detailed discussion relating to switching surges and related issues was presented, and a detailed simulation study was performed to determine peak surge levels. It is concluded that line energization surges in the system modeled here are well within limits, since peak SSF determined is less than 2.0 p.u. Also, line energization surges originating from remote substations are found to be severer than those originating locally. For the latter case, the arrester installed at that location does not have a large impact on the surges.

It is also seen that critical length of a transmission line can be distributed among multiple lines terminated at the same node; it doesn't have to be concentrated in one single stretch. In most cases this distribution does not translate to a simple addition of individual line lengths, for example, if the number of lines connected at a node is more than two. This length is influenced by conductor arrangement and tower geometry.

Since lightning surges were not studied in this thesis, the author advises the reader and the utility company to conduct appropriate investigations for the same. Often, lightning surges do more harm than switching surges. It will be beneficial to study the peak lightning surge in the model developed here and analyze any necessary protective measures.

5.2 Future work

The following scope exists for future work in this thesis:

- A more realistic picture of the system can be captured if the 230 kV lines are modeled in greater detail, along with all surge protection devices present in substations modeled in chapter-4.
- Other generating stations can be included to incorporate accurate information relating to 500 kV sources. In the simulations presented in this report, the source was assumed to be located at Palo Verde substation at all times and this bus was modeled as an infinite bus. Including other generating stations can be beneficial, especially if it is required to study peak SSFs at any other 500 kV or 230 kV substation.
- Various other switching scenarios can be simulated to study transient overvoltage at other substation buses.
- Further scope exists to carry out this study by simulating lightning surges. Peak surge values at various buses can be determined using similar simulations as described in this thesis. And then protection against lightning surges can be studied using the same surge arrester models as those used here.

REFERENCES

- [1] Mariano G. Ippolito, Fabio M., Guiseppe M., Rossano M., “No load energization of very long EHV mixed overhead-cable lines”, *University Paris-Est Creteil, 45th International*, September 2010.
- [2] Bozidar Filipovic-Grcic´, Ivo Uglesic, Ivica Pavic, “Application of line surge arresters for voltage uprating and compacting of overhead transmission lines” *Elsevier Electric Power Systems Research*, May 2016.
- [3] P. Bunov, L. Klingbeil, James Hunt, A. J. F. Keri et al, “Transmission line arresters’ application for control of switching overvoltages on 500 kV transmission line”, *T&D Conference and Exposition*, 2014 IEEE PES.
- [4] Y. Pencheng, C. Shuiming, HE Jinliang, “Effect of different arresters on switching overvoltages is UHV transmission lines”, *Tsinghua Science and Technology*, pp. 325-328, Volume 15, issue 3, June 2010.
- [5] R. Shariatinasab, B. Vahidi, S. H. Hosseinian, A. Ametani, “Application of ANN and genetic algorithm for evaluation the optimum location of arresters on power networks due to the switching overvoltages”, *Journal of Energy, CIGRE conference*, Croatia, 2008, page 10-15.
- [6] S. Venkatesan, A. Haddad, H. Griffiths et al., “Reducing air clearance requirements for voltage uprating of overhead line by use of line surge arresters”, 2009, pp 224-229.
- [7] R. Shariatinasab, B. Vahidi, S. H. Hosseinian, A. Ametani, “Probabilistic evaluation of optimal location of surge arresters on EHV and UHV networks due to switching and lightning surges”, *IEEE Transactions on Power Delivery*, Vol 24 no. 4, October 2009.
- [8] Jorge C. P. Vieira, Milton E. Z. Alcahuaman, “Methods of transient overvoltage suppression caused by energizing maneuver on a transmission line a little greater than the half wavelength (HWL+)”, *INTERCON, IEEE XXIII International Congress*, August 2016.
- [9] F.S. Prabhakara, K. Parthasarathy and H.N. Ramachandra Rao. “Analysis of Natural Half-Wave-Length Power Transmission Lines”. *IEEE Transactions on Power Apparatus and Systems*, vol. PAS 88, N° 12 , pp. 1787 – 1794, December 1969.
- [10] Portela, C., “Non-Conventional AC Solutions Adequate for Very Long Distance Transmission”, Proc. In XI Symposium of Specialists in Electric Operational and Expansion Planning, Belém, Brazil, 17 – 20 March, 2009.
- [11] H. Seyedi, M. Sanaye-Pasand, M. R. Dadashzadeh, “Application of transmission line surge arresters to reduce switching overvoltages”, *International Conference on Power Systems Transients*, Montreal, Canada, June 19-23 2005.

- [12] Ivo Uglešić, Božidar Filipović-Grčić, Srećko Bojić, “Transients caused by uncontrolled and controlled switching of circuit breakers”, *The International Symposium on High Voltage Technique “Hofler’s Days”*, November 2013, Slovenia.
- [13] Koki Aodsup, T. Kulworawanichpong, “Numerical modeling and very fast transient simulation of MOV surge arresters”, *Power and Energy Engineering Conference (APPEEC), 2012 Asia-Pacific*.
- [14] V. S. Brito, George R. S. Lira et al., “A wide-range model for metal oxide surge arrester”, *IEEE Transactions on Power Delivery, Vol:PP, Issue 99*, May 2017.
- [15] Lars Liljestränd, Elisabeth Lindell, “Efficiency of surge arresters as protective devices against circuit breaker induced overvoltages”, *IEEE Transactions on Power Delivery, Vol 31, Issue 4*, August 2016.
- [16] Leela A. M., V. Muralidhara, K. N. Ravi, N. Vasudev, R. S. S. Aradhya, “Study of high frequency characteristics of metal oxide surge arrester”, *International Conference*, 2015.
- [17] C62.11-2012 - IEEE Standard for Metal-Oxide Surge Arresters for AC Power Circuits (>1 kV), December 2012 (<https://ieeexplore.ieee.org/stamp/stamp.jsp?tp=&arnumber=6392178>).
- [18] Pablo Mourente Miguel, “Comparison of surge arrester models”, *IEEE Transactions on Power Delivery, Vol 29, Issue 1*, February 2014.
- [19] P. F. Evangelides, C. A. Christodoulou et al., “Parameters’ selection for metal oxide surge arresters models using genetic algorithm”, *30th International Conference on Lightning Protection, ICLP*, Cagliari, Italy, September 2010.
- [20] H. Zeinoddini-Meymand, Behrooz Vahidi et al., “Optimal surge arrester parameter evaluation using a PSO-based multiobjective approach”, *IEEE Transactions on Power Delivery, Vol 28, Issue 3*, July 2013.
- [21] Nicolae Tarfulea, Doru Vatau, Florin Balcu et al., “A new algorithm for the design of metal oxide varistor surge arresters”, *IEEE 16th International Conference on Environmental and Electrical Engineering (EEEIC)*, June 2016.
- [22] Afshin Rezaei-Zare, “Equivalent winding capacitance network for transformer transient analysis based on standard test data”, *IEEE Transactions on Power Delivery, Vol 32, No. 4*, August 2017.
- [23] Das, J. C. *Transients in Electrical Systems: Analysis, Recognition, and Mitigation*. New York: McGraw-Hill, 2010.
- [24] IEC-60071-4:2004 – Computational guide to insulation coordination and modelling of electrical networks (https://webstore.iec.ch/preview/info_iec60071-4%7Bed1.0%7Den.pdf).

- [25] IEEE Std 1427-2006 – IEEE Guide for Recommended Electrical Clearances and Insulation Levels in Air Insulated Electrical Power Systems. IEEE Standard for High-Voltage Testing Techniques," in IEEE Std 4-2013, vol. no. pp.1-213.